

Two Gluon Production and Longitudinal Correlations in the Color Glass Condensate

Kenji Fukushima

*Yukawa Institute for Theoretical Physics, Kyoto University, Oiwake-cho,
Kitashirakawa, Sakyo-ku, Kyoto 606-8502, Japan*

Yoshimasa Hidaka

*RIKEN BNL Research Center, Brookhaven National Laboratory,
Upton, New York 11973, USA*

Abstract

We derive an analytical expression for the two-gluon multiplicity in the pA (light-heavy) collisions, and focus specifically on the rapidity dependent part. We approximate the gauge field from the heavy target as the Color Glass Condensate which interacts with the light projectile whose source density allows for a perturbative expansion. We discuss the longitudinal correlations of produced particles. Our calculation goes in part beyond the eikonal limit for the emitted gluons so that we can retain the exponential terms with respect to the rapidity difference. Our expression can thus describe the short-range correlations as well as the long-range ones for which our formula is reduced to the known expression. In a special case of two high- p_t gluons in the back-to-back kinematics we find that dependence on the rapidity separation is only moderate even in the diagrammatically connected part.

1 Introduction

The gluon distribution function in hadrons grows up at high collision energy and thus small Bjorken's x , which makes it indispensable to elaborate a resummation over the multiple scattering to abundant soft gluons. When the transverse distribution of partons is saturated eventually at small x and small Q^2 [1], the classical approximation is to be a good description of the hadron wave-function dominated by coherent small- x partons. In fact, a shift in the perturbative QCD vacuum by such a classical field is an efficient prescription

to take account of dense gluons within the eikonal approximation. This resummation scheme has been well founded in the non-linear but still perturbative regime embodied by the notion of the Color Glass Condensate (CGC) [2,3].

We are interested in the single and two gluon production in the CGC formalism in this paper. It is not quite viable to solve the non-linear problem fully in the case that both the target and the projectile have dense gluon contents. In contrast, the analytical calculation is feasible [4] if we deal with the asymmetric case of a light projectile scattering off a heavy target, as is the case in the pA collision or in the forward and backward rapidity regions in the AA collision. The present work aims to elucidate the production rate of two gluons having two distinct rapidities y_1 and y_2 in the asymmetric collisions. We have to limit the separation $|y_1 - y_2|$ parametrically less than $1/\alpha_s$ since we do not take account of quantum evolution which is incorporated by the radiative corrections between two separate gluons. It is maybe worth noting that we can describe another effect of quantum evolution with respect to the hadron wave-function by evolution of the saturation scale [5] though it is non-trivial whether and how these quantum corrections are to be factorized [6].

We shall accomplish the whole calculation of the two-gluon production along the line of Refs. [4,7] and thus our results should be an extension of that given in Ref. [8] where $y_1 \gg y_2$ is assumed for simplicity. Our results are in fact consistent with Ref. [9] in the eikonal limit that emitted gluons are energetic enough to overwhelm the transverse recoil, but they possess intricate extra contributions depending on $\Delta y = y_1 - y_2$. We will later discuss what the missing part was that causes the discrepancy.

It should be an important problem to clarify the particle correlation reflecting the parton saturation effect. This is because the CGC configuration naturally leads to strong chromo-electric and chromo-magnetic fields which extend between the target and the projectile [10,11]. It would be conceivable that the longitudinal correlation provides us with information on the initial dense state to be regarded as CGC matter.

Moreover, in Ref. [12], the jet azimuthal back-to-back correlation has been considered, which is also discussed in Refs. [9,13]. Also, from different interest, the recent experimental data at RHIC (Relativistic Heavy-Ion Collider) exhibits the wide rapidity correlation in the near side of the trigger and associated jets, which could have an influential remnant from the initial state and the strong color field in it [14,15]. In a different context, in Refs. [16,17], the forward-backward correlation has been discussed which seems to have a direct link to the longitudinal field presumably existing in CGC matter. All these preceding efforts are decent to motivate us to carry out the analytical QCD evaluation in the same procedure as Ref. [4] where only minimal assumptions under theoretical control hide behind modeling.

In the subsequent sections we shall elucidate the two-gluon multiplicity starting with the established computation for the single-gluon case for self-contained discussions.

2 Gluon Production

We here make a quick review on the formulation to evaluate the gluon production amplitude, which should be useful for clarity of our convention adopted in the present paper.

2.1 One gluon production

The production amplitude of one on-shell gluon with three-momentum \mathbf{p} , helicity λ , and color a is expressed as the amplitude from the physical vacuum $|\Omega\rangle$ to the single-gluon asymptotic state $|\mathbf{p}, \lambda, a\rangle$. Using the Lehmann-Symanzik-Zimmermann (LSZ) reduction formula [18], we can generally write this amplitude in a form of

$$\langle \mathbf{p}; \lambda, a | \Omega \rangle = i \epsilon_{\mu}^{(\lambda)}(\mathbf{p}) \int d^4x e^{ip \cdot x} \square_x \langle \Omega | A_a^{\mu}(x) | \Omega \rangle, \quad (1)$$

where $A_a^{\mu}(x)$ denotes the gluon field operator. We note that we should take the on-shell limit $p_0 \rightarrow E_p = |\mathbf{p}|$ in the right-hand side because the emitted gluon is real hence on-shell. The phase space integral and the summation over physical degrees of freedom lead us to the following expression for the multiplicity of emitted gluons per rapidity;

$$\left\langle \frac{dN_g}{dy} \right\rangle = \frac{1}{4\pi} \int \frac{d^2\mathbf{p}_{\perp}}{(2\pi)^2} \sum_{\lambda, a} \langle |\langle \mathbf{p}; \lambda, a | \Omega \rangle|^2 \rangle. \quad (2)$$

Here we have introduced the momentum rapidity variable as $y \equiv \frac{1}{2} \ln[p^+/p^-]$ where $p^{\pm} \equiv (p^0 \pm p^z)/\sqrt{2}$ which can be expressed as $|\mathbf{p}_{\perp}| e^{\pm y}/\sqrt{2}$ by using the on-shell condition, i.e. $2p^+p^- = |\mathbf{p}_{\perp}|^2$. It is then straightforward to confirm that the phase space integral is rewritten as $d^3\mathbf{p}/[(2\pi)^3 2E_p] = dy d^2\mathbf{p}_{\perp}/[2(2\pi)^3]$. In Eq. (2) the summation with respect to λ should run over only the transverse components corresponding to physical degrees of freedom, and $\langle \cdots \rangle$ denotes an average over the color configuration of sources.

It is convenient to adopt the following convention to define the physical polarization in the light-cone coordinates [19]. Let us particularly consider the light-cone gauge defined by

$$n_{\mu} A^{\mu} = A^+ = 0, \quad (3)$$

where $n_\mu \equiv \delta_\mu^+$. Then, as beautifully demonstrated in Refs. [7,20], we can take advantage of this gauge choice to reduce computational cost significantly. The light-cone gauge condition leads to $\epsilon^{(\lambda)+} = 0$ and there are not four but three independent polarization vectors, two of whose linear combinations are physical. The following projection operator enables us to identify the transverse parts simply with $\lambda = 1, 2$, that is,

$$\epsilon_\mu^{(\lambda)}(p) \equiv -D_{\mu\lambda}(p), \quad (4)$$

where

$$D_{\mu\nu}(p) \equiv -g_{\mu\nu} + \frac{n_\mu p_\nu + n_\nu p_\mu}{n \cdot p} - \frac{p^2}{(n \cdot p)^2} n_\mu n_\nu. \quad (5)$$

The above tensor structure appears also in the gluon propagator in the light-cone gauge. It is important to note that these polarization vectors are doubly transverse to both the momentum and gauge directions, i.e.

$$p^\mu \epsilon_\mu^{(\lambda)}(p) = 0, \quad n^\mu \epsilon_\mu^{(\lambda)}(p) = 0. \quad (6)$$

Moreover, using the explicit form of Eqs. (4) and (5), we can show that the sum over physical polarization amounts to

$$\sum_{\lambda=1,2} \epsilon_\mu^{(\lambda)}(p) \epsilon_\nu^{(\lambda)}(p) = D_{\mu\nu}(p). \quad (7)$$

Since the above is multiplied by A^μ and A^ν after all (see Eq. (1)), only a quantity of $A^\mu D_{\mu\nu} A^\nu$ is necessary to reach the final expression. This quantity is reduced to as simple as $A^i A^i$ owing to the gauge condition (3). Therefore, we only have to retain a δ_{ij} term out of $D_{\mu\nu}(p)$ in the polarization summation to estimate the one gluon production. Consequently the gluon multiplicity is expressed as

$$\left\langle \frac{dN_g}{dy} \right\rangle = \frac{1}{4\pi} \int \frac{d^2 \mathbf{p}_\perp}{(2\pi)^2} (p^2)^2 \langle \mathcal{A}_a^{i*}(p) \mathcal{A}_a^i(p) \rangle, \quad (8)$$

where we have denoted the vacuum expectation value of the gauge field, i.e. background gauge field, as $\mathcal{A}_a^\mu(x) \equiv \langle \Omega | A_a^\mu(x) | \Omega \rangle$. Because p^2 in Eq. (8) is a four-momentum squared, only the singular contribution proportional to $1/p^2$ in $\mathcal{A}_a^i(p)$ remains non-vanishing in the on-shell limit that we should take in the end. We note that we define the Fourier transformation in our convention as

$$\mathcal{A}_a^i(p) \equiv \int d^4x e^{ip \cdot x} \mathcal{A}_a^i(x). \quad (9)$$

Generally this is a complex-valued function and satisfies $\mathcal{A}_a^{i*}(p) = \mathcal{A}_a^i(-p)$.

2.2 Two gluon production

It is a straightforward generalization to continue on considering not only single but also the multiple gluon production in this way. We will focus particularly on the two-gluon case in this work, though it is in principle possible to accommodate more gluons. In the same way as previously explained, we can write down the production amplitude for two gluons with three-momenta \mathbf{p} , \mathbf{q} , helicity λ , σ , and color a , b , respectively. The LSZ reduction formula yields the amplitude as

$$\begin{aligned} & \langle \mathbf{p}, \lambda, a; \mathbf{q}, \sigma, b | \Omega \rangle \\ &= i \epsilon_{\mu}^{(\lambda)}(\mathbf{p}) \int d^4x e^{ip \cdot x} \square_x i \epsilon_{\nu}^{(\sigma)}(\mathbf{q}) \int d^4y e^{iq \cdot y} \square_y \langle \Omega | T[A_a^{\mu}(x) A_b^{\nu}(y)] | \Omega \rangle. \end{aligned} \quad (10)$$

Here T represents the time ordering as usual. From this amplitude we can reach an expression for the two-gluon multiplicity for one emitted with rapidity y_1 and the other emitted with rapidity y_2 ;

$$\begin{aligned} \left\langle \frac{dN_{\text{gg}}}{dy_1 dy_2} \right\rangle &= \frac{1}{16\pi^2} \int \frac{d^2\mathbf{p}_{\perp}}{(2\pi)^2} \frac{d^2\mathbf{q}_{\perp}}{(2\pi)^2} \sum_{\lambda, \sigma, a, b} \langle |\langle \mathbf{p}, \lambda, a; \mathbf{q}, \sigma, b | \Omega \rangle|^2 \rangle \\ &= \left\langle \frac{dN_{\text{g}}}{dy_1} \frac{dN_{\text{g}}}{dy_2} \right\rangle + \frac{1}{16\pi^2} \int \frac{d^2\mathbf{p}_{\perp}}{(2\pi)^2} \frac{d^2\mathbf{q}_{\perp}}{(2\pi)^2} (p^2)^2 (q^2)^2 \langle 2\text{Re}[\mathcal{A}_a^{*i}(p) \mathcal{G}_{ab}^{ij}(p, q) \mathcal{A}_b^{*j}(q)] \rangle \\ &\quad + \frac{1}{16\pi^2} \int \frac{d^2\mathbf{p}_{\perp}}{(2\pi)^2} \frac{d^2\mathbf{q}_{\perp}}{(2\pi)^2} (p^2)^2 (q^2)^2 \langle \mathcal{G}_{ba}^{\dagger ji}(q, p) \mathcal{G}_{ab}^{ij}(p, q) \rangle. \end{aligned} \quad (11)$$

The first term corresponds to a long-range correlation part which is not suppressed for large $|y_1 - y_2|$. This term is important to consider the azimuthal angle correlation, which is contributed through the average over the configuration of the sources [15]. The second is an interference term, and the third is a short-range correlation part which depends on Δy as diminishing as $|\Delta y|$ goes large. To extract the connected contribution henceforth, we have defined the propagator and its Fourier transform as follows;

$$\mathcal{G}_{ab}^{\mu\nu}(x, y) \equiv \langle \Omega | T[A_a^{\mu}(x) A_b^{\nu}(y)] | \Omega \rangle - \mathcal{A}_a^{\mu}(x) \mathcal{A}_b^{\nu}(y), \quad (12)$$

$$\mathcal{G}_{ab}^{\mu\nu}(p, q) \equiv \int d^4x d^4y e^{ip \cdot x + iq \cdot y} \mathcal{G}_{ab}^{\mu\nu}(x, y). \quad (13)$$

Just for clarity we remark that $\mathcal{G}_{ba}^{\dagger ji}(q, p)$ literally means $\mathcal{G}_{ab}^{*ij}(p, q)$. The central discussion in what follows lies in analytical evaluation of the background gauge field in the CGC formalism and the associated propagator on top of the background.

We can pictorially visualize these three terms enumerated in Eq. (11) in a way as sketched in Fig. 1. The first (disconnected), the second (interference), and the third (connected) terms of Eq. (11) correspond to Figs. 1 (A), (B), and

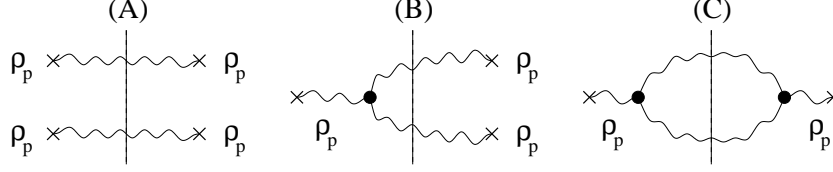


Fig. 1. Diagrammatic representation of three distinct contributions to the two-gluon production: (A) the disconnected $\mathcal{O}(\rho_p^4)$ diagram, (B) the interference $g\mathcal{O}(\rho_p^3)$ one, and (C) the connected $g^2\mathcal{O}(\rho_p^2)$ one.

(C), respectively. The cross represents the interaction with the light projectile whose intrinsic color distribution is regarded as small perturbation, i.e. $\rho_p = \mathcal{O}(g)$. As a result of this setting (A), (B), and (C) have the same order; (A) = $\mathcal{O}(\rho_p^4)$, (B) = $g\mathcal{O}(\rho_p^3)$, (C) = $g^2\mathcal{O}(\rho_p^2)$, and they are all $\mathcal{O}(g^4)$. We can drop (B) under an assumption of the Gaussian average over ρ_p . Although the long-range correlation stemming from (A), which is predominant in the AA collision, is physically interesting [15,16,21], we will not consider (A) and concentrate in (C) only that is the contribution carrying the short-range correlations like $e^{\pm\Delta y}$. In fact, what we will pursue in this work is to retrieve the neglected rapidity dependence in the two-gluon production with emphasis on the analytical formulation. We will discuss the full correlation including (A) and phenomenological implication in a separate publication.

3 Background Gauge Field with Dense-Dilute Sources

We shall adopt the CGC picture to proceed to concrete calculations. The background field originates from the dense color distribution inside a fast-moving hadron. In a classical approximation in which quantum corrections (i.e. the wave-function renormalization to the field expectation value) are neglected, $\mathcal{A}^\mu(x)$ is simply a solution to the classical Yang-Mills equations of motion with color source $\rho_A(\mathbf{x}_\perp)$. This type of the one-source problem is solvable and the explicit form of $\mathcal{A}^\mu(x)$ as a function of $\rho_A(\mathbf{x}_\perp)$ is known [22].

In this paper, as we mentioned in Introduction, we shall consider a situation with two color sources corresponding to asymmetric collisions; one source distribution is dense from a heavy nuclei which gives the color current $J^- = \delta(x^+)\rho_A(\mathbf{x}_\perp)$ and the other is dilute from a proton for instance, which gives $J^+ = \delta(x^-)\rho_p(\mathbf{x}_\perp)$. We treat $\rho_p(\mathbf{x}_\perp)$ as small perturbation, where we should note that the classical approximation still works because of the presence of large $\rho_A(\mathbf{x}_\perp)$.

Here, these naïve color currents do not satisfy the covariant conservation. We

thus need to augment these definitions with appropriate gauge rotations as

$$J_a^- = \delta(x^+) V_{ab}(x) \rho_{Ab}(\mathbf{x}_\perp), \quad J_a^+ = \delta(x^-) U_{ab}(x) \rho_{pb}(\mathbf{x}_\perp), \quad (14)$$

where $V(x) = \mathcal{P}_{x^-} \exp[ig \int^{x^-} dz^- A^+]$ and $U(x) = \mathcal{P}_{x^+} \exp[ig \int^{x^+} dz^+ A^-]$ with \mathcal{P}_{x^\pm} being the path-ordering with respect to x^\pm . The color matrices A^\pm are the full gauge fields (including both classical and quantum parts) in the color adjoint representation. The covariant conservation is then manifest because $D^+ V(x) = 0$ and $D^- U(x) = 0$.

The analytical calculation makes sense when either $\rho_A(\mathbf{x}_\perp)$ or $\rho_p(\mathbf{x}_\perp)$ is small compared to the gluon transverse momentum (i.e. saturation scale). We can then perform the perturbative expansion in terms of small $\rho_p(\mathbf{x}_\perp)$. The gauge field associated with such an asymmetric collision can have an expansion like

$$\mathcal{A}^\mu = \mathcal{A}_{(0)}^\mu + \mathcal{A}_{(1)}^\mu + \cdots, \quad (15)$$

where $\mathcal{A}_{(0)}^\mu$ and $\mathcal{A}_{(1)}^\mu$ are the zeroth and first order terms with respect to $\rho_p(\mathbf{x}_\perp)$, respectively. One can in principle continue the expansion up to arbitrary order, but what we need to retain in this work is only up to the first order. In this formalism of the pA problem the gauge fields become time independent after interaction at the collision point, as we will see shortly. The LSZ formula means that the residue of the massless pole corresponds to the gluon number associated with the gauge fields in the asymptotic state. This makes a contrast to the approximate prescription often used in the AA case; the field amplitude for each momentum mode translates into the particle number, which could depend on time [23]. It is not clear how the LSZ formula works for the AA case, in particular in the expanding geometry, while it has no ambiguity in the pA collisions.

3.1 Gauge choice

It is practically crucial to take an appropriate gauge choice to make the whole computational procedure transparent. In what follows, we will make use of the light-cone (LC) gauge $A^+ = 0$ with the background field $\mathcal{A}_{(0)}^\mu$ which is usually referred to as a solution in the covariant (COV) gauge,

$$\mathcal{A}_{(0)}^+ = 0, \quad \mathcal{A}_{(0)}^- = -\frac{1}{\partial_\perp^2} \delta(x^+) \rho_A(\mathbf{x}_\perp), \quad \mathcal{A}_{(0)}^i = 0. \quad (16)$$

It should be mentioned that $V(x) = 1$ in this $A^+ = 0$ gauge so that no complication enters involving $\rho_A(\mathbf{x}_\perp)$, which is a great advantage in this technique. In contrast to that, even in the leading order in $\rho_p(\mathbf{x}_\perp)$ at the classical level, we have to keep $U(x)$ which stems from nonzero $\mathcal{A}_{(0)}^-$. Because $\mathcal{A}_{(0)}^-$ has $\delta(x^+)$

in it, the x^+ dependence of $U(x)$ is given as

$$U(x) = \begin{cases} 1 & \text{for } x^+ < 0, \\ U(\mathbf{x}_\perp) \equiv \mathcal{P}_{x^+} \exp \left[ig \int_{0^-}^{0^+} dx^+ \mathcal{A}_{(0)}^- \right] & \text{for } x^+ \geq 0^+. \end{cases} \quad (17)$$

We will use the same notation for $U(x)$ and $U(\mathbf{x}_\perp)$ hoping that no confusion would arise from this. We remark that the integration with respect to x^+ in the exponential needs a careful treatment with appropriate regularization [4,24,25].

To reiterate explicitly, our choice (that was first adopted in Ref. [7]) is

$$\mathcal{A}^\mu = \underbrace{\mathcal{A}_{(0)}^\mu}_{\text{COV for A}} + \underbrace{\mathcal{A}_{(1)}^\mu}_{\text{LC for p}}. \quad (18)$$

The essential point in this trick invented in Ref. [7] is that the classical solution in the COV gauge for left-moving $\rho_A(\mathbf{x}_\perp)$ is consistent with the LC gauge for right-moving $\rho_p(\mathbf{x}_\perp)$. Actually, since $\mathcal{A}_{(0)}^+ = 0$, the solution (16) obtained in the COV gauge for $\rho_A(\mathbf{x}_\perp)$ may well be regarded as a solution in the LC gauge for $\rho_p(\mathbf{x}_\perp)$. [Usually $\mathcal{A}_{(0)}^+ = 0$ is *assumed* in addition to the gauge fixing condition.]

The benefits from the choice (18) are twofold: One is understood from Eq. (7), that is, the light-cone gauge significantly simplifies the summation over physical degrees of freedom. The other is the fact that only one component of the background field (16) is non-vanishing and the remaining $\mathcal{A}_{(0)}^-$ takes a finite value at $x^+ = 0$ only. Therefore the gluon propagation receives no effect from the background field except at $x^+ = 0$ where the eikonal phase and color rotation are induced. This nice feature tremendously reduces the computational labor.

3.2 Classical solution

We are evaluating $\mathcal{A}_{(1)}^\mu$ that is necessary not only for the single-gluon production but also for the two-gluon production multiplicity. From the equations of motion, $D_\mu F^{\mu\nu} = J^\nu$, in the light-cone gauge we have a set of equations to determine $\mathcal{A}_{(1)}^\mu$, that is,

$$-\partial^{+2} \mathcal{A}_{(1)}^- + \partial^+ \partial^i \mathcal{A}_{(1)}^i = J^+, \quad (19)$$

$$\partial^+ D_{(0)}^- \mathcal{A}_{(1)}^- - \partial_\perp^2 \mathcal{A}_{(1)}^- + D_{(0)}^- \partial^i \mathcal{A}_{(1)}^i - 2ig[\partial^i \mathcal{A}_{(0)}^-, \mathcal{A}_{(1)}^i] = 0, \quad (20)$$

$$2\partial^+ D_{(0)}^- \mathcal{A}_{(1)}^i - \partial^+ \partial^i \mathcal{A}_{(1)}^- - \partial_\perp^2 \mathcal{A}_{(1)}^i + \partial^i \partial^j \mathcal{A}_{(1)}^j = 0, \quad (21)$$

for $\nu = +, -, i$, respectively. It is notable that J^- disappears in the second equation. Using Eq. (19) we can simplify Eq. (20) into

$$\square \mathcal{A}_{(1)}^- - 2ig[\mathcal{A}_{(0)}^-, \partial^+ \mathcal{A}_{(1)}^-] - 2ig[\partial^i \mathcal{A}_{(0)}^-, \mathcal{A}_{(1)}^i] = 0. \quad (22)$$

Here we used $D_{(0)}^- J^+ = 0$. In the same way Eq. (21) becomes as simple as

$$\square \mathcal{A}_{(1)}^i - 2ig[\mathcal{A}_{(0)}^-, \partial^+ \mathcal{A}_{(1)}^i] = -\frac{\partial^i}{\partial^+} J^+. \quad (23)$$

It is not difficult to solve Eq. (23) for $\mathcal{A}_{(1)}^i$ with the initial boundary condition,

$$\mathcal{A}_{(1)}^i(x^+ < 0, x^-, \mathbf{x}_\perp) = \theta(x^-) \frac{\partial^i}{\partial_\perp^2} \rho_p(\mathbf{x}_\perp), \quad (24)$$

which is nothing but a retarded solution in the presence of one right-moving source before the collision.

Let us then examine the connection condition across the singularity located at $x^+ = 0$. By integrating Eq. (23) with respect to x^+ from 0^- to 0^+ , and picking up a singularity contained in $\mathcal{A}_{(0)}^-$ (see Eq. (16)), we can acquire the boundary condition,

$$\int_{0^-}^{0^+} dx^+ D_{(0)}^- \mathcal{A}_{(1)}^i = 0. \quad (25)$$

Here we have dropped the overall ∂^+ which is irrelevant. We immediately see the solution to the above equation to be

$$\mathcal{A}_{(1)}^i(x^+ = 0^+, x^-, \mathbf{x}_\perp) = U(\mathbf{x}_\perp) \mathcal{A}_{(1)}^i(x^+ = 0^-, x^-, \mathbf{x}_\perp), \quad (26)$$

remembering that $D^- U(x) = 0$. In the forward light-cone region, i.e. $x^+ > 0$, there is no background field and thus the gluon propagation is expressed by the retarded free propagator Δ_R defined by $\square_x \Delta_R(x) = i\delta^{(4)}(x)$ leading to

$$\Delta_R(x) = \int \frac{d^4 p}{(2\pi)^4} \frac{-i}{p^2 + ip^+ \epsilon} e^{-ip \cdot x}. \quad (27)$$

Here $\epsilon \rightarrow 0^+$ is understood as usual. It is easy to make sure that Δ_R is nonzero only for $x^+ > 0$. It is straightforward to confirm from the above definition a useful relation,

$$\partial^+ \Delta_R(x) \Big|_{x^+=0^+} = \frac{i}{2} \delta(x^-) \delta^{(2)}(\mathbf{x}_\perp). \quad (28)$$

Then the solution to Eq. (23) at nonzero x^+ is generally to be expressed as

$$\mathcal{A}_{(1)}^i = \mathcal{A}_{(1)<}^i + \mathcal{A}_{(1)>}^i \quad (29)$$

with

$$\mathcal{A}_{(1<)}^i(x) = \theta(-x^+)\theta(x^-)\frac{\partial^i}{\partial_\perp^2}\rho_p(\mathbf{x}_\perp), \quad (30)$$

$$\begin{aligned} \mathcal{A}_{(1>)}^i(x) = & \int_{y^+>0} d^4y \left[-i\Delta_R(x-y) \right] \left[-\frac{\partial_y^i}{\partial_y^+} J^+(y) \right] \\ & + \int dy^- d^2\mathbf{y}_\perp \left[-2i\partial_x^+ \Delta_R(x-y) \right] \mathcal{A}_{(1)}^i(y) \Big|_{y^+=0^+}. \end{aligned} \quad (31)$$

Here $\mathcal{A}_{(1<)}^i$ is the past solution coming from the source for $x^+ < 0$. The first term in $\mathcal{A}_{(1>)}^i$ has the same origin but it involves a color rotation by $U(\mathbf{x}_\perp)$ additionally for $x^+ > 0$. In the presence of the second term $\mathcal{A}_{(1>)}^i$ satisfies the correct boundary condition (26) in the $x^+ \rightarrow 0^+$ limit, which is obvious from Eq. (28). Also we can readily find that this second term produces no contribution for $x^+ > 0$ when acted by the d'Alembertian \square . From these expressions we can operate the d'Alembertian to find

$$\square \mathcal{A}_{(1<)}^i = -2\delta(x^+)\delta(x^-)\frac{\partial^i}{\partial_\perp^2}\rho_p(\mathbf{x}_\perp) - \theta(-x^+)\theta(x^-)\partial^i\rho_p(\mathbf{x}_\perp), \quad (32)$$

$$\square \mathcal{A}_{(1>)}^i = 2\delta(x^+)\delta(x^-)U(\mathbf{x}_\perp)\frac{\partial^i}{\partial_\perp^2}\rho_p(\mathbf{x}_\perp) - \theta(x^+)\theta(x^-)\partial^i[U(\mathbf{x}_\perp)\rho_p(\mathbf{x}_\perp)]. \quad (33)$$

We can take the Fourier transform and reach

$$-p^2 \mathcal{A}_{(1<)}^i(p) = -ip^i \left[\frac{p^2}{(p^+ + i\epsilon)(p^- - i\epsilon)} \right] \frac{\rho_p(\mathbf{p}_\perp)}{\mathbf{p}_\perp^2}, \quad (34)$$

$$-p^2 \mathcal{A}_{(1>)}^i(p) = -i \int \frac{d^2\mathbf{k}_{1\perp}}{(2\pi)^2} \left[\frac{p^i \mathbf{k}_{1\perp}^2}{(p^+ + i\epsilon)(p^- + i\epsilon)} - 2k_1^i \right] U(\mathbf{k}_{2\perp}) \frac{\rho_p(\mathbf{k}_{1\perp})}{\mathbf{k}_{1\perp}^2}, \quad (35)$$

where $\mathbf{k}_{1\perp} + \mathbf{k}_{2\perp} = \mathbf{p}_\perp$. We can compute the single-gluon multiplicity by substituting the sum of the above expressions into Eq. (8) and taking an ensemble average over the $\rho_p(\mathbf{x}_\perp)$ and $\rho_A(\mathbf{x}_\perp)$ distributions. We will not do that because the final results are known [4,26] and the physical quantity of our current interest is the two-gluon multiplicity.

Although it is not relevant to the single-gluon case, the two-gluon production requires the functional form of $\mathcal{A}_{(1)}^-$ for the present purpose to evaluate the two-gluon production. This is actually where our results come to differ from Ref. [9]. There is no source contribution $\propto J^\mu$ in $\mathcal{A}_{(1)}^-$. From Eq. (22) the boundary condition is inferred from

$$\int_{0^-}^{0^+} dx^+ \left(D_{(0)}^- \mathcal{A}_{(1)}^- - ig \left[\partial^i \mathcal{A}_{(0)}^-, \frac{1}{\partial^+} \mathcal{A}_{(1)}^i \right] \right) = 0, \quad (36)$$

where we have dropped the overall ∂^+ in the same way as previously. The

above leads to the connection condition as

$$\begin{aligned} \mathcal{A}_{(1)}^-(x^+ = 0^+, x^-, \mathbf{x}_\perp) &= U(\mathbf{x}_\perp) \mathcal{A}_{(1)}^-(x^+ = 0^-, x^-, \mathbf{x}_\perp) \\ &+ \left[\partial^i U(\mathbf{x}_\perp) \right] \frac{1}{\partial^+} \mathcal{A}_{(1)}^i(x^+ = 0^-, x^-, \mathbf{x}_\perp). \end{aligned} \quad (37)$$

The first term in the right-hand side is zero in fact because $\mathcal{A}_{(1)}^-(x^+ = 0^-) = 0$. Nevertheless, we write it to avoid confusion in order to define a convenient notation M_ν^μ in later discussions. The solution for arbitrary x^+ is, therefore, given as

$$\mathcal{A}_{(1<)}^-(x) = 0, \quad (38)$$

$$\mathcal{A}_{(1>)}^-(x) = \int dy^- d^2 \mathbf{y}_\perp \left[-2i \partial_x^+ \Delta_R(x - y) \right] \mathcal{A}_{(1)}^-(y) \Big|_{y^+ = 0^+}. \quad (39)$$

The representation in momentum space is thus $\mathcal{A}_{(1<)}^-(p) = 0$ and

$$-p^2 \mathcal{A}_{(1>)}^-(p) = -i \int \frac{d^2 \mathbf{k}_{1\perp}}{(2\pi)^2} \frac{-2\mathbf{k}_{1\perp} \cdot \mathbf{k}_{2\perp}}{p^+ + i\epsilon} U(\mathbf{k}_{2\perp}) \frac{\rho_p(\mathbf{k}_{1\perp})}{\mathbf{k}_{1\perp}^2}, \quad (40)$$

where $\mathbf{k}_{1\perp} + \mathbf{k}_{2\perp} = \mathbf{p}_\perp$ again. We note that the right-hand side has no dependence on p^- because $\square \mathcal{A}_{(1>)}^-$ is proportional to $\delta(x^+)$. For consistency check one can readily see that $\mathcal{A}_{(1>)}^i$ and $\mathcal{A}_{(1>)}^-$ obtained above certainly satisfy the rest of the equations of motion, namely, Eq. (19) as they should.

Later on, for notational simplicity, we will introduce M_ν^μ and C^μ to express the connection condition and the solution, respectively.

4 Propagator with the Background Gauge Field

It is the background propagator that is necessary for the two-gluon multiplicity. We will calculate it here by means of the expansion in terms of small $\mathcal{A}_{(1)}^\mu \propto \rho_p$. The full background propagator without expansion is defined by

$$-i \left[D^\lambda D_\lambda g_{\mu\nu} - D_\mu D_\nu - 2ig F_{\mu\nu} \right]_x \mathcal{G}^{\nu\sigma}(x, y) = g_\mu^\sigma \delta^{(4)}(x - y), \quad (41)$$

where both $\mathcal{A}_{(0)}^-$ and $\mathcal{A}_{(1)}^\mu$ enter the background field. We will use the adjoint matrix notation from now on, namely, a color matrix is understood as

$$(\mathcal{A}^\mu)_{ab} = (T_A^c \mathcal{A}_c^\mu)_{ab} \equiv if^{acb} \mathcal{A}_c^\mu, \quad (42)$$

in the color adjoint representation. Then, the quantity in the square brackets is decomposed into the zeroth-order and first-order parts with respect to $\mathcal{A}_{(1)}^\mu$.

It follows that we have

$$\begin{aligned} D^\lambda D_\lambda g_{\mu\nu} - D_\mu D_\nu - 2igF_{\mu\nu} \\ = D_{(0)}^\lambda D_{(0)\lambda} g_{\mu\nu} - D_{(0)\mu} D_{(0)\nu} - 2igF_{(0)\mu\nu} + i\delta\Gamma_{\mu\nu} + \mathcal{O}(\rho_p^2), \end{aligned} \quad (43)$$

where we have defined the vertex matrix of order $\mathcal{O}(\rho_p)$ as follows;

$$i\delta\Gamma_{\mu\nu} \equiv -ig \left\{ \left[(\partial_\lambda \mathcal{A}_{(1)}^\lambda) + 2\mathcal{A}_{(1)}^\lambda \partial_\lambda \right] g_{\mu\nu} + 2(\partial_\mu \mathcal{A}_{(1)\nu}) - 2(\partial_\nu \mathcal{A}_{(1)\mu}) \right\}. \quad (44)$$

We remark that we have dropped terms irrelevant to the gluon propagator, that means, terms which vanish when sandwiched by the zeroth-order propagator with transversality and also with the upper + components vanishing due to gauge fixing. We shall define the zeroth-order background propagator as

$$-i \left[D_{(0)}^\lambda D_{(0)\lambda} g_{\mu\nu} - D_{(0)\mu} D_{(0)\nu} - 2igF_{(0)\mu\nu} \right]_x \mathcal{G}_{(0)}^{\nu\sigma}(x, y) = g_\mu^\sigma \delta^{(4)}(x - y), \quad (45)$$

and then we can express the full propagator in Eq. (41) in a way as $\mathcal{G} = (\mathcal{G}_{(0)}^{-1} + \delta\Gamma)^{-1}$, that yields an expansion,

$$\mathcal{G}^{\mu\nu}(x, y) = \mathcal{G}_{(0)}^{\mu\nu}(x, y) - \int d^4z \mathcal{G}_{(0)}^{\mu\lambda}(x, z) \delta\Gamma_{\lambda\sigma}(z) \mathcal{G}_{(0)}^{\sigma\nu}(z, y) + \mathcal{O}(\rho_p^2). \quad (46)$$

At this stage it is tangible how we dropped terms from Eq. (43) to Eq. (44); irrelevant terms in $\delta\Gamma_{\mu\nu}$, in fact, arise from the transverse properties, i.e., $n_\mu \mathcal{G}_{(0)}^{\mu\nu} = 0$ and $\partial_\mu \mathcal{G}_{(0)}^{\mu\nu} = 0$ (see also Eq. (6)). In momentum space we can write the vertex as

$$\delta\Gamma_{\mu\nu}(p, q) = ig\mathcal{A}_{(1)}^\lambda(p + q)\Gamma_{\mu\lambda\nu}(p, q) \quad (47)$$

with

$$\Gamma_{\mu\lambda\nu}(p, q) = (p - q)_\lambda g_{\mu\nu} + 2q_\mu g_{\nu\lambda} - 2p_\nu g_{\lambda\mu}. \quad (48)$$

It should be mentioned that the above vertex is slightly different from a standard three-point QCD vertex. It might seem that the momentum conservation does not hold. This is because q_ν out of $-2p_\nu - q_\nu$ vanishes from $q_\nu \mathcal{G}_{(0)}^{\nu\rho}(q) = 0$ and p_μ out of $2q_\mu + p_\mu$ vanishes from $\mathcal{G}_{(0)}^{\rho\mu}(p)p_\mu = 0$. All the terms involving $\mathcal{A}_{(0)}^-$ disappear due to gauge fixing. We shall then concretely compute Eq. (46) in the subsequent subsections below.

4.1 $\mathcal{G}_{(0)}^{\mu\nu}(x, y)$ for $(x^+ > 0, y^+ > 0)$ or $(x^+ < 0, y^+ < 0)$

Now let us calculate the propagator in the region without crossing the source singularity, that is, the region with $x^+ > 0$ and $y^+ > 0$ or the region with $x^+ < 0$ and $y^+ < 0$ as depicted in Fig. 2 (A). There, the background propagator is just the free one which is unity in color space given by

$$-i \left[(\partial^\lambda \partial_\lambda) g_{\mu\nu} - (\partial_\mu \partial_\nu) \right]_x \Delta^{\nu\sigma}(x, y) = g_\mu^\sigma \delta^{(4)}(x - y). \quad (49)$$

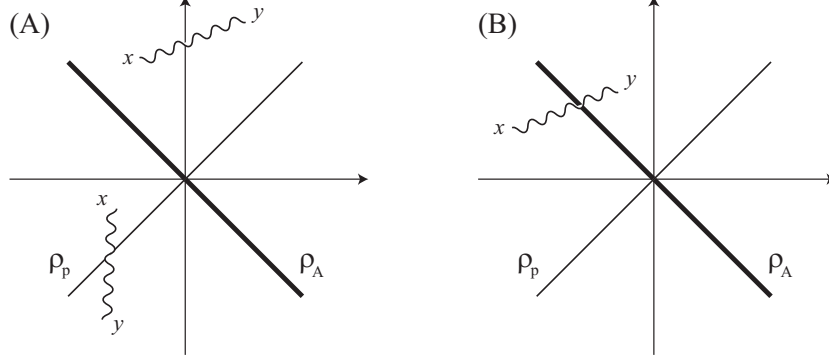


Fig. 2. Some typical examples for $\mathcal{G}_{(0)}^{\mu\nu}(x, y)$: (A) The propagation is free from the source singularity in the case for $(x^+ < 0, y^+ < 0)$ or $(x^+ > 0, y^+ > 0)$. (B) The singularity at $x^+ = 0$ affects the propagation which occurs in the case for $(x^+ < 0, y^+ > 0)$ or $(x^+ > 0, y^+ < 0)$.

In the momentum representation, we can write the time-ordered propagator in a concise form as

$$\Delta^{\mu\nu}(p, q) \equiv (2\pi)^4 \delta^{(4)}(p + q) \frac{iD^{\mu\nu}(p)}{p^2 + i\epsilon}, \quad (50)$$

using $D^{\mu\nu}(p)$ defined in Eq. (5). The standard ϵ prescription enables us to define the retarded ($x^+ > y^+$) and advanced ($x^+ < y^+$) propagators, i.e., $\Delta_R^{\mu\nu}(p, q)$ and $\Delta_A^{\mu\nu}(p, q)$ by replacement of the denominator by $p^2 + i\epsilon p^+$ and $p^2 - i\epsilon p^+$, respectively.

4.2 $\mathcal{G}_{(0)}^{\mu\nu}(x, y)$ for $(x^+ < 0 < y^+)$ or $(y^+ < 0 < x^+)$

As a preparation to proceed to the case with a singularity at $x^+ = 0$ on the propagating path, we shall introduce the following notation. We will express the boundary conditions, Eq. (26) and Eq. (37), into a single form of

$$A^\mu(x^+ = 0^+) = M^\mu_\nu A^\nu(x^+ = 0^-), \quad (51)$$

where the gauge rotation associated with the singularity is

$$\begin{aligned} M_j^i &= \delta_j^i U(\mathbf{x}_\perp), \quad M_-^- = U(\mathbf{x}_\perp), \quad M_i^- = \partial^i U(\mathbf{x}_\perp) \frac{1}{\partial^+}, \\ M_-^i &= M_+^i = 0, \quad M_+^- = 0, \quad M_\mu^+ = 0. \end{aligned} \quad (52)$$

This representation is useful in the following formulation.

If $x^+ < 0 < y^+$ or $y^+ < 0 < x^+$ then the propagator passes over the source singularity. We show an example in Fig. 2 (B). We will derive the appropriate boundary condition at the singularity here. To do so, we shall pick up only ∂^-

and $\delta(x^+)$ terms from the equations of motion. Then we consider the connection condition for each polarization component μ for the case of $y^+ < 0 < x^+$ first. From the boundary condition for the gauge field (51) it is straightforward to write the boundary condition down for the propagator as well in a similar form as

$$\mathcal{G}_{(0)}^{\mu\nu}(x, y) \Big|_{x^+=0^+} = M^\mu_\sigma \Delta^{\sigma\nu}(x, y) \Big|_{x^+=0^-}. \quad (53)$$

We note that the free propagator appears in the right-hand side for $x^+ = 0^-$ and $y^+ < 0$. Using the same technique as in the previous section where we calculated the gauge field, we can express the propagator for $y^+ < 0 < x^+$ with satisfying the above boundary condition as

$$\begin{aligned} \mathcal{G}_{(>)}^{\mu\nu}(x, y) &= \int dz^- d^2 \mathbf{z}_\perp \left[-2i\partial_x^+ \Delta_R^{\mu\lambda}(x, z) \right] g_{\lambda\sigma} \mathcal{G}_{(0)}^{\sigma\nu}(z, y) \Big|_{z^+=0^+} \\ &= - \int dz^- d^2 \mathbf{z}_\perp \left[-2i\partial_x^+ \Delta_R^{\mu i}(x, z) \right] U(\mathbf{z}_\perp) \Delta^{i\nu}(z, y) \Big|_{z^+=0}. \end{aligned} \quad (54)$$

In the momentum representation the above translates into

$$\begin{aligned} \mathcal{G}_{(>)}^{\mu\nu}(p, q) &= \int d^4 x d^4 y e^{ip \cdot x + iq \cdot y} \mathcal{G}_{(>)}^{\mu\nu}(x, y) \theta(-y^+) \\ &= (2\pi) \delta(p^+ + q^+) \theta(p^+) \frac{2p^+ D^{\mu\lambda}(p) D_\lambda^\nu(q)}{(p^2 + i\epsilon p^+)(q^2 - i\epsilon q^+)} U(\mathbf{p}_\perp + \mathbf{q}_\perp). \end{aligned} \quad (55)$$

Here we note that the propagator poles are located only on the lower (or upper) half plane in terms of the complex p^- (or q^- respectively) variable, which reflects the boundary condition, $y^+ < 0 < x^+$.

Similarly, the propagator for $x^+ < 0 < y^+$ is to be written as

$$\mathcal{G}_{(<)}^{\mu\nu}(p, q) = (2\pi) \delta(p^+ + q^+) \theta(q^+) \frac{2q^+ D^{\mu\lambda}(p) D_\lambda^\nu(q)}{(p^2 - i\epsilon p^+)(q^2 + i\epsilon q^+)} U^\dagger(-\mathbf{p}_\perp - \mathbf{q}_\perp), \quad (56)$$

in momentum space. We note that the color rotation takes place in the opposite orientation (i.e. $U^{-1} = U^\dagger$) to the previous case because the gluon propagation penetrates into the source from the opposite side.

4.3 Propagator and Amplitude

We now get ready to proceed to evaluating the expanded propagator (46). The most general form is, however, not necessary for the two-gluon production amplitude. In coordinate space only the late time behavior at $x^+ \gg 0$ and $y^+ \gg 0$ is relevant to the production process. We can actually confirm that the production amplitude does not have any contribution from the region where x^+ and y^+ are negative. In the following argument, thus, we shall restrict the time arguments as positive x^+ and y^+ only.

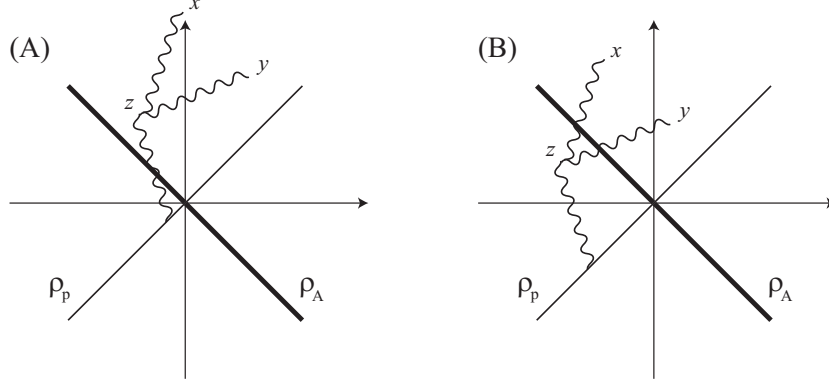


Fig. 3. Typical diagrams representing the first-order propagator which contributes to the two-gluon production amplitude: (A) One gluon splits into two after interaction with the target. (B) Two gluons receive interaction with the target.

The production process can be separated into two distinct types according to the location of the three-point vertex. Figure 3 is the diagrammatic representation for them. We can distinguish (A) and (B) out of Eq. (46) by the sign of z^+ so that we can decompose it into

$$\begin{aligned} \mathcal{G}^{\mu\nu}(x, y) - \mathcal{G}_{(0)}^{\mu\nu}(x, y) = & - \int d^4z \Delta^{\mu\lambda}(x, z) \delta\Gamma_{(>)\lambda\sigma}(z) \Delta^{\sigma\nu}(z, y) \\ & - \int d^4z \mathcal{G}_{(>)}^{\mu\lambda}(x, z) \delta\Gamma_{(<)\lambda\sigma}(z) \mathcal{G}_{(<)}^{\sigma\nu}(z, y), \end{aligned} \quad (57)$$

where we can forget about $\mathcal{G}_{(0)}^{\mu\nu}(x, y)$ for our purpose. In the above we have defined,

$$\delta\Gamma_{(>)\lambda\sigma}(z) \equiv \delta\Gamma_{\lambda\sigma}(z)\theta(z^+), \quad \delta\Gamma_{(<)\lambda\sigma}(z) \equiv \delta\Gamma_{\lambda\sigma}(z)\theta(-z^+). \quad (58)$$

This relatively simple form of Eq. (57) is, as we stated above, valid under the condition, $x^+ > 0$ and $y^+ > 0$. The first and second lines correspond to (A) and (B) of Fig. 3, respectively.

4.4 Evaluating $\Delta^{\mu\lambda} \delta\Gamma_{(>)\lambda\sigma} \Delta^{\sigma\nu}$

First we shall explicitly evaluate the contribution at $z^+ > 0$ shown in Fig. 3 (A). Since the expression in momentum space is necessary to acquire the amplitude, let us take the Fourier transform,

$$\begin{aligned} \int d^4x d^4y e^{ip \cdot x + iq \cdot y} \theta(x^+) \theta(y^+) \int d^4z \Delta^{\mu\lambda}(x, z) \delta\Gamma_{(>)\lambda\sigma}(z) \Delta^{\sigma\nu}(z, y) \\ = -\theta(p^+) \theta(q^+) \frac{D^{\mu\lambda}(p) \delta\Gamma_{(>)\lambda\sigma}(p, q) D^{\sigma\nu}(q)}{(p^2 + i\epsilon)(q^2 + i\epsilon)}, \end{aligned} \quad (59)$$

where we have used $p^+ > 0$ and $q^+ > 0$ in the denominator. From Eq. (10) the matrix element $\langle \mathbf{p}, \lambda, a; \mathbf{q}, \sigma, b | \Omega \rangle$ turns out to have a contribution as

$$\langle \mathbf{p}, \lambda, a; \mathbf{q}, \sigma, b | \Omega \rangle_{(>)} = -\epsilon_\mu^{(\lambda)}(\mathbf{p}) \epsilon_\nu^{(\sigma)}(\mathbf{q}) \delta\Gamma_{(>)}^{\mu\nu}(p, q). \quad (60)$$

Using Eqs. (10), (35), (40), and (47) we can figure its explicit form out as

$$\begin{aligned} & \langle \mathbf{p}, \lambda, a; \mathbf{q}, \sigma, b | \Omega \rangle_{(>)} \\ &= g \epsilon_\mu^{(\lambda)}(\mathbf{p}) \epsilon_\nu^{(\sigma)}(\mathbf{q}) \int \frac{d^2 \mathbf{k}_{1\perp}}{(2\pi)^2} T_{(>)}^{\mu\nu}(p, q; \mathbf{k}_{1\perp}, \mathbf{k}_{2\perp}) \left[U(\mathbf{k}_{2\perp}) \frac{\rho_p(\mathbf{k}_{1\perp})}{\mathbf{k}_{1\perp}^2} \right]^{ab}, \end{aligned} \quad (61)$$

where $\mathbf{k}_{1\perp} + \mathbf{k}_{2\perp} = \mathbf{p}_\perp + \mathbf{q}_\perp$ and we have defined as follows;

$$T_{(>)}^{\mu\nu}(p, q; \mathbf{k}_{1\perp}, \mathbf{k}_{2\perp}) \equiv \frac{D^{\mu\lambda'}(p) \Gamma_{\lambda'\delta\sigma'}(p, q) D^{\sigma'\nu}(q)}{(p+q)^2 + i(p^+ + q^+)\epsilon} C^\delta(p+q; \mathbf{k}_{1\perp}, \mathbf{k}_{2\perp}). \quad (62)$$

Here, we have defined

$$\begin{aligned} C^+(p, \mathbf{k}_{1\perp}, \mathbf{k}_{2\perp}) &= 0, \\ C^-(p, \mathbf{k}_{1\perp}, \mathbf{k}_{2\perp}) &= \frac{-2\mathbf{k}_{1\perp} \cdot \mathbf{k}_{2\perp}}{p^+ + i\epsilon}, \\ C^i(p, \mathbf{k}_{1\perp}, \mathbf{k}_{2\perp}) &= \frac{p^i \mathbf{k}_{1\perp}^2}{(p^+ + i\epsilon)(p^- + i\epsilon)} - 2k_1^i. \end{aligned} \quad (63)$$

so that we can express the gauge field after the collision in a concise form as

$$-p^2 \mathcal{A}_{(1>)}^\mu(p) = -i \int \frac{d^2 \mathbf{k}_{1\perp}}{(2\pi)^2} C^\mu(p; \mathbf{k}_{1\perp}, \mathbf{k}_{2\perp}) U(\mathbf{k}_{2\perp}) \frac{\rho_p(\mathbf{k}_{1\perp})}{\mathbf{k}_{1\perp}^2}. \quad (64)$$

4.5 Evaluating $\mathcal{G}_{(>)}^{\mu\lambda} \delta\Gamma_{(<)\lambda\sigma} \mathcal{G}_{(<)}^{\sigma\nu}$

In the same way we can continue the calculation by taking the Fourier transformation to obtain,

$$\begin{aligned} & \int d^4x d^4y e^{ip \cdot x + iq \cdot y} \theta(x^+) \theta(y^+) \int d^4z \mathcal{G}_{(>)}^{\mu\lambda}(x, z) \delta\Gamma_{(<)\lambda\sigma}(z) \mathcal{G}_{(<)}^{\sigma\nu}(z, y) \\ &= \int \frac{d^4k_1}{(2\pi)^4} \frac{d^4k_2}{(2\pi)^4} \mathcal{G}_{(>)}^{\mu\lambda}(p, -k_1) \delta\Gamma_{(<)\lambda\sigma}(k_1, k_2) \mathcal{G}_{(<)}^{\lambda\nu}(-k_2, q). \end{aligned} \quad (65)$$

By substituting the explicit forms given by Eqs. (55) and (56) we can write the above down explicitly as

$$\begin{aligned}
& \int \frac{d^4 k_1}{(2\pi)^4} \frac{d^4 k_2}{(2\pi)^4} \mathcal{G}_{(>)}^{\mu\lambda}(p, -k_1) \delta\Gamma_{(<)\lambda\sigma}(k_1, k_2) \mathcal{G}_{(<)}^{\lambda\nu}(-k_2, q) \\
&= \frac{\theta(p^+)}{p^2 + i\epsilon p^+} \cdot \frac{\theta(q^+)}{q^2 + i\epsilon q^+} \int \frac{d^4 k_1}{(2\pi)^4} \frac{d^4 k_2}{(2\pi)^4} (2\pi)\delta(p^+ - k_1^+) (2\pi)\delta(-k_2^+ + q^+) \\
&\quad \times \frac{2k_1^+ D^{\mu\alpha}(p) D_\alpha^\lambda(k_1)}{(k_1^2 + i\epsilon)} \cdot \frac{2k_2^+ D^{\sigma\beta}(k_2) D_\beta^\nu(q)}{(k_2^2 + i\epsilon)} \\
&\quad \times U(\mathbf{p}_\perp - \mathbf{k}_{1\perp}) \delta\Gamma_{(<)\lambda\sigma}(k_1, k_2) U^\dagger(\mathbf{q}_\perp - \mathbf{k}_{2\perp}).
\end{aligned} \tag{66}$$

The poles in $\delta\Gamma_{(<)\lambda\sigma}(k_1, k_2)$ in the complex k_1^- and k_2^- plane are found on the upper half plane. We can then perform the integration with respect to k_1^- and k_2^- avoiding the pole in $\delta\Gamma_{(<)\lambda\sigma}(k_1, k_2)$, so that we pick up the contributions $-(2\pi i)(2k_1^+)^{-1}\delta(k_1^- - \mathbf{k}_{1\perp}^2/(2k_1^+))$ from $1/k_1^2$ and $-(2\pi i)(2k_2^+)^{-1}\delta(k_2^- - \mathbf{k}_{2\perp}^2/(2k_2^+))$ from $1/k_2^2$, which leads to

$$\begin{aligned}
& \int \frac{d^4 k_1}{(2\pi)^4} \frac{d^4 k_2}{(2\pi)^4} \mathcal{G}_{(>)}^{\mu\lambda}(p, -k_1) \delta\Gamma_{(<)\lambda\sigma}(k_1, k_2) \mathcal{G}_{(<)}^{\lambda\nu}(-k_2, q) \\
&= -\frac{\theta(p^+)}{p^2 + i\epsilon p^+} \cdot \frac{\theta(q^+)}{q^2 + i\epsilon q^+} \int \frac{d^2 \mathbf{k}_{1\perp}}{(2\pi)^2} \frac{d^2 \mathbf{k}_{2\perp}}{(2\pi)^2} D^{\mu\alpha}(p) D_\alpha^\lambda(k_1) D^{\sigma\beta}(k_2) D_\beta^\nu(q) \\
&\quad \times U(\mathbf{p}_\perp - \mathbf{k}_{1\perp}) \delta\Gamma_{(<)\lambda\sigma}(k_1, k_2) U^\dagger(\mathbf{k}_{2\perp} - \mathbf{q}_\perp),
\end{aligned} \tag{67}$$

after the integration with respect to k_1^\pm and k_2^\pm . Here the delta functions impose that $k_1^2 = k_2^2 = 0$, $k_1^+ = p^+$, and $k_2^+ = q^+$. From Eq. (10) the matrix element from this contribution becomes

$$\begin{aligned}
\langle \mathbf{p}, \lambda, a; \mathbf{q}, \sigma, b | \Omega \rangle_{(<)} &= -\epsilon_\mu^{(\lambda)}(\mathbf{p}) \epsilon_\nu^{(\sigma)}(\mathbf{q}) \int \frac{d^2 \mathbf{k}_{1\perp}}{(2\pi)^2} \frac{d^2 \mathbf{k}_{2\perp}}{(2\pi)^2} D^{\mu\lambda'}(k_1) D^{\sigma'\nu}(k_2) \\
&\quad \times U(\mathbf{p}_\perp - \mathbf{k}_{1\perp}) \delta\Gamma_{(<)\lambda'\sigma'}(k_1, k_2) U^\dagger(\mathbf{k}_{2\perp} - \mathbf{q}_\perp),
\end{aligned} \tag{68}$$

which simplifies further to be

$$\begin{aligned}
\langle \mathbf{p}, \lambda, a; \mathbf{q}, \sigma, b | \Omega \rangle_{(<)} &= g \epsilon_\mu^{(\lambda)}(\mathbf{p}) \epsilon_\nu^{(\sigma)}(\mathbf{q}) \int \frac{d^2 \mathbf{k}_{1\perp}}{(2\pi)^2} \frac{d^2 \mathbf{k}_{2\perp}}{(2\pi)^2} \\
&\quad \times \left[U(\mathbf{p}_\perp - \mathbf{k}_{1\perp}) \frac{\rho_p(\mathbf{k}_{1\perp} + \mathbf{k}_{2\perp})}{(\mathbf{k}_{1\perp} + \mathbf{k}_{2\perp})^2} U^\dagger(\mathbf{k}_{2\perp} - \mathbf{q}_\perp) \right]^{ab} T_{(<)}^{\mu\nu}(p, q; \mathbf{k}_{1\perp}, \mathbf{k}_{2\perp}).
\end{aligned} \tag{69}$$

where we have defined

$$T_{(<)}^{\mu\nu}(p, q; \mathbf{k}_{1\perp}, \mathbf{k}_{2\perp}) \equiv \frac{D^{\mu\lambda'}(k_1) \Gamma_{\lambda' i \sigma'}(k_1, k_2) D^{\sigma'\nu}(k_2) (k_1 + k_2)^i}{(p^+ + q^+ + i\epsilon)(k_1^- + k_2^- - i\epsilon)}. \tag{70}$$

Here we recall that $k_1^- = \mathbf{k}_{1\perp}^2/2p^+$ and $k_2^- = \mathbf{k}_{2\perp}^2/2q^+$ from the on-shell condition.

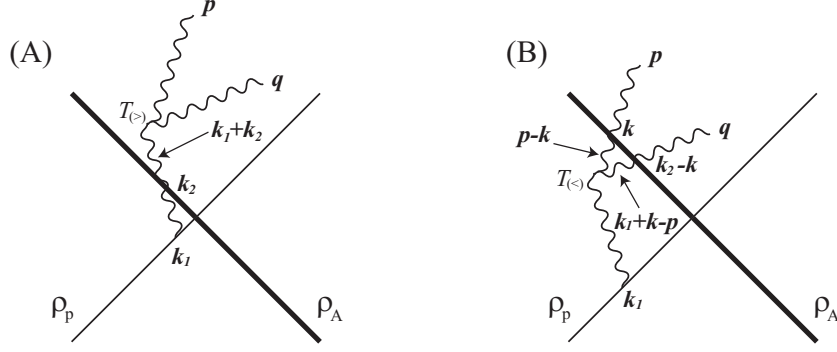


Fig. 4. Momentum assignment for (A) $\langle \mathbf{p}, \mathbf{q} | \Omega \rangle_{(>)}$ and (B) $\langle \mathbf{p}, \mathbf{q} | \Omega \rangle_{(<)}$ respectively.

For later convenience we shall shift the momenta as

$$\mathbf{k}_{1\perp} \rightarrow \mathbf{k}'_{1\perp} = \mathbf{k}_{1\perp} + \mathbf{k}_{2\perp}, \quad \mathbf{k}_{2\perp} \rightarrow \mathbf{k}'_{2\perp} = \mathbf{p}_{\perp} - \mathbf{k}'_{1\perp} + \mathbf{k}_{2\perp}, \quad (71)$$

and omit the prime on the momenta afterward. Then, the above amplitude is rewritten into

$$\begin{aligned} \langle \mathbf{p}, \lambda, a; \mathbf{q}, \sigma, b | \Omega \rangle_{(<)} &= g \epsilon_{\mu}^{(\lambda)}(\mathbf{p}) \epsilon_{\nu}^{(\sigma)}(\mathbf{q}) \int \frac{d^2 \mathbf{k}_{1\perp}}{(2\pi)^2} \frac{d^2 \mathbf{k}_{\perp}}{(2\pi)^2} \\ &\times T_{(<)}^{\mu\nu}(p, q; \mathbf{p}_{\perp} - \mathbf{k}_{\perp}, \mathbf{k}_{1\perp} + \mathbf{k}_{\perp} - \mathbf{p}_{\perp}) \left[U(\mathbf{k}_{\perp}) \frac{\rho_p(\mathbf{k}_{1\perp})}{\mathbf{k}_{1\perp}^2} U^{\dagger}(\mathbf{k}_{\perp} - \mathbf{k}_{2\perp}) \right]^{ab}. \end{aligned} \quad (72)$$

4.6 Total amplitude

After all, the sum of Eqs. (61) and (72) amounts to the total amplitude,

$$\begin{aligned} \langle \mathbf{p}, \lambda, a; \mathbf{q}, \sigma, b | \Omega \rangle &= g \epsilon_{\mu}^{(\lambda)}(\mathbf{p}) \epsilon_{\nu}^{(\sigma)}(\mathbf{q}) \int \frac{d^2 \mathbf{k}_{1\perp}}{(2\pi)^2} \frac{\rho_p^c(\mathbf{k}_{1\perp})}{\mathbf{k}_{1\perp}^2} \\ &\times \left[T_{(>)}^{\mu\nu}(p, q; \mathbf{k}_{1\perp}, \mathbf{k}_{2\perp}) T_A^d U^{dc}(\mathbf{k}_{2\perp}) + \int \frac{d^2 \mathbf{k}_{\perp}}{(2\pi)^2} \right. \\ &\times T_{(<)}^{\mu\nu}(p, q; \mathbf{p}_{\perp} - \mathbf{k}_{\perp}, \mathbf{k}_{1\perp} + \mathbf{k}_{\perp} - \mathbf{p}_{\perp}) U(\mathbf{k}_{\perp}) T_A^c U^{\dagger}(\mathbf{k}_{\perp} - \mathbf{k}_{2\perp}) \left. \right]^{ab}. \end{aligned} \quad (73)$$

Figure 4 shows the momentum assignment overlaid on Fig. 3. In the above expression the $SU(N_c)$ algebra in the adjoint representation is denoted by T_A . Let us now confirm that this results are certainly reduced to zero in the limit of vanishing target source, that is, $U(\mathbf{k}_{\perp}) \rightarrow (2\pi)^2 \delta^{(2)}(\mathbf{k}_{\perp})$, for consistency check.

Then, the quantity inside the square brackets is

$$T_A^c \left[T_{(>)}^{\mu\nu}(p, q; \mathbf{p}_{\perp} + \mathbf{q}_{\perp}, \mathbf{0}_{\perp}) + T_{(<)}^{\mu\nu}(p, q; \mathbf{p}_{\perp}, \mathbf{q}_{\perp}) \right]. \quad (74)$$

After some calculations we can find that

$$\begin{aligned} T_{(>)}^{\mu\nu}(p, q; \mathbf{p}_\perp + \mathbf{q}_\perp, \mathbf{0}_\perp) &= -T_{(<)}^{\mu\nu}(p, q; \mathbf{p}_\perp, \mathbf{q}_\perp) \\ &= \frac{D^{\mu\lambda}(p)\Gamma_{\lambda i\sigma}(p, q)D^{\sigma\nu}(q)(p^i + q^i)}{(p^+ + q^+)(p^- + q^-)}, \end{aligned} \quad (75)$$

which makes Eq. (74) canceled as anticipated.

For later convenience let us write Eq. (73) in a slightly different way. Noting that,

$$\int \frac{d^2\mathbf{k}_\perp}{(2\pi)^2} U(\mathbf{k}_\perp) T_A^c U^\dagger(\mathbf{k}_\perp - \mathbf{k}_{2\perp}) = T_A^d U^{dc}(\mathbf{k}_{2\perp}), \quad (76)$$

we can rewrite the first and second terms altogether as

$$\begin{aligned} &\langle \mathbf{p}, \lambda, a; \mathbf{q}, \sigma, b | \Omega \rangle \\ &= g \epsilon_\mu^{(\lambda)}(\mathbf{p}) \epsilon_\nu^{(\sigma)}(\mathbf{q}) \int \frac{d^2\mathbf{k}_{1\perp}}{(2\pi)^2} \frac{\rho_p^c(\mathbf{k}_{1\perp})}{\mathbf{k}_{1\perp}^2} \int \frac{d^2\mathbf{k}_\perp}{(2\pi)^2} \left[U(\mathbf{k}_\perp) T_A^c U^\dagger(\mathbf{k}_\perp - \mathbf{k}_{2\perp}) \right]^{ab} \\ &\quad \times \left[T_{(>)}^{\mu\nu}(p, q; \mathbf{k}_{1\perp}, \mathbf{k}_{2\perp}) + T_{(<)}^{\mu\nu}(p, q; \mathbf{p}_\perp - \mathbf{k}_\perp, \mathbf{k}_{1\perp} + \mathbf{k}_\perp - \mathbf{p}_\perp) \right]. \end{aligned} \quad (77)$$

This is a useful form because, as we will face soon below, the sum of two terms in the angle brackets has partial cancellation in some cases.

5 Rapidity Correlation

Now that we have worked out the amplitude, its squared quantity immediately leads us to an expression for the correlation function shown in Fig. 1 (C) (i.e. connected diagram), that is,

$$\begin{aligned} \left\langle \frac{dN_{\text{gg}}}{dy_1 dy_2} \right\rangle_{\text{conn}} &= \frac{g^2}{16\pi^2} \int \frac{d^2\mathbf{p}_\perp}{(2\pi)^2} \frac{d^2\mathbf{q}_\perp}{(2\pi)^2} \frac{d^2\mathbf{k}_{1\perp}}{(2\pi)^2} \frac{d^2\mathbf{k}'_{1\perp}}{(2\pi)^2} \frac{\langle \rho_p^a(\mathbf{k}_{1\perp}) \rho_p^{a'*}(\mathbf{k}'_{1\perp}) \rangle}{\mathbf{k}_{1\perp}^2 \mathbf{k}'_{1\perp}^2} \\ &\times \left\{ \text{tr}[T_{(>)} \cdot T_{(>)}^\dagger] \langle U^{ba}(\mathbf{k}_{2\perp}) U^{\dagger a'b'}(\mathbf{k}'_{2\perp}) \text{tr}[T_A^b T_A^{b'}] \rangle \right. \\ &\quad + \int \frac{d^2\mathbf{k}_\perp}{(2\pi)^2} \text{tr}[T_{(<)} \cdot T_{(>)}^\dagger] \langle \text{tr}[U(\mathbf{k}_\perp) T_A^a U^\dagger(\mathbf{k}_\perp - \mathbf{k}_{2\perp}) T_A^{b'}] U^{\dagger a'b'}(\mathbf{k}'_{2\perp}) \rangle \\ &\quad + \int \frac{d^2\mathbf{k}'_\perp}{(2\pi)^2} \text{tr}[T_{(>)} \cdot T_{(<)}^\dagger] \langle U^{ba}(\mathbf{k}_{2\perp}) \text{tr}[T_A^b U(\mathbf{k}'_\perp - \mathbf{k}'_{2\perp}) T_A^{a'} U^\dagger(\mathbf{k}'_\perp)] \rangle \\ &\quad + \int \frac{d^2\mathbf{k}_\perp}{(2\pi)^2} \frac{d^2\mathbf{k}'_\perp}{(2\pi)^2} \text{tr}[T_{(<)} \cdot T_{(<)}^\dagger] \\ &\quad \times \left. \langle \text{tr}[U(\mathbf{k}_\perp) T_A^a U^\dagger(\mathbf{k}_\perp - \mathbf{k}_{2\perp}) U(\mathbf{k}'_\perp - \mathbf{k}'_{2\perp}) T_A^{a'} U^\dagger(\mathbf{k}'_\perp)] \rangle \right\}, \end{aligned} \quad (78)$$

where we have suppressed the momentum arguments for $T_{(>)}^{\mu\nu} \equiv T_{(>)}^{\mu\nu}(p, q; \mathbf{k}_{1\perp}, \mathbf{k}_{2\perp})$, $T_{(>)}^{\dagger\mu\nu} \equiv T_{(>)}^{\dagger\mu\nu}(p, q; \mathbf{k}'_{1\perp}, \mathbf{k}'_{2\perp})$, $T_{(<)}^{\mu\nu} \equiv T_{(<)}^{\mu\nu}(p, q; \mathbf{p}_\perp - \mathbf{k}_\perp, \mathbf{k}_{1\perp} + \mathbf{k}_\perp - \mathbf{p}_\perp)$, and $T_{(<)}^{\dagger\mu\nu} \equiv T_{(<)}^{\dagger\mu\nu}(p, q; \mathbf{p}_\perp - \mathbf{k}'_\perp, \mathbf{k}'_{1\perp} + \mathbf{k}'_\perp - \mathbf{p}_\perp)$. We note that $\mathbf{k}_{2\perp}$ and $\mathbf{k}'_{2\perp}$ are defined through $\mathbf{k}_{1\perp} + \mathbf{k}_{2\perp} = \mathbf{k}'_{1\perp} + \mathbf{k}'_{2\perp} = \mathbf{p}_\perp + \mathbf{q}_\perp$. These are our final results. We present the results by somewhat more intuitive expressions in terms of the gluon distribution functions in Appendix A. The evaluation for the Wilson line average is supplemented in Appendix B.

In the rest of this section we further explore the rapidity correlation out of Eq. (78) in some special situations. First, let us consider the remaining correlation which is rapidity independent in the long range. We assumed $|\Delta y| < 1/\alpha_s$ to avoid the quantum evolution effect, as we mentioned in Introduction. Now we shall consider the correlation in the rapidity region satisfying $1 \ll |\Delta y| < 1/\alpha_s$, so that the eikonal approximation can work for emitted gluons. Then, we set $y_2 \gg 1$ and $y_1 \ll -1$ and regard q^+ and p^- as much greater than other scales.

In this approximation it is immediate to see;

$$\begin{aligned} (p+q)^2 &\approx 2q^+p^-, \\ C^-(p+q, \mathbf{k}_{1\perp}, \mathbf{k}_{2\perp}) &\approx 0, \quad C^i(p+q, \mathbf{k}_{1\perp}, \mathbf{k}_{2\perp}) \approx -2k^i, \\ \Gamma_{\mu\lambda\nu}(p, q) &\approx q^+(-g_{+\lambda}g_{\mu\nu} + 2g_{+\mu}g_{\nu\lambda}), \end{aligned} \quad (79)$$

where we have dropped two terms from $\Gamma_{\mu\lambda\nu}(p, q)$ because no finite contribution arises whenever either of μ , λ , or ν takes $+$. After some calculations with using the on-shell conditions we can find $T_{(>)}^{ij}$ and $T_{(<)}^{ij}$ to be rewritten as

$$T_{(>)}^{ij}(p, q; \mathbf{k}_{1\perp}, \mathbf{k}_{2\perp}) \approx \frac{4p^i k_1^j}{\mathbf{p}_\perp^2} = -\frac{4\pi \mathbf{k}_{1\perp}^2}{g^2} f^i(\mathbf{p}_\perp) f^j(\mathbf{k}_{1\perp}), \quad (80)$$

$$T_{(<)}^{ij}(p, q; \mathbf{p}_\perp - \mathbf{k}_\perp, \mathbf{k}_{1\perp} + \mathbf{k}_\perp - \mathbf{p}_\perp) \approx \frac{-4(p-k)^i k_1^j}{(\mathbf{p}_\perp - \mathbf{k}_\perp)^2} = \frac{4\pi \mathbf{k}_{1\perp}^2}{g^2} f^i(\mathbf{p}_\perp - \mathbf{k}_\perp) f^j(\mathbf{k}_{1\perp}), \quad (81)$$

where we define f^i following the notation in Ref. [9] by

$$f^i(\mathbf{p}_\perp) = \frac{-ig}{\sqrt{\pi}} \frac{p^i}{\mathbf{p}_\perp^2}. \quad (82)$$

We note that $f^i(\mathbf{k}_{1\perp})\rho_p(\mathbf{k}_{1\perp})$ is nothing but the perturbative Weizsäcker-Williams gluon field. From a different point of view, the above together with $\epsilon_i^{(\lambda)}(\mathbf{p})$ can be interpreted as coming from the amplitude of the soft gluon emission in the color dipole picture.

After all, the total amplitude becomes as simple as

$$\begin{aligned} \langle \mathbf{p}, i, a; \mathbf{q}, j, b | \Omega \rangle = & -\frac{4\pi}{g} \int \frac{d^2 \mathbf{k}_{1\perp}}{(2\pi)^2} f^j(\mathbf{k}_{1\perp}) \rho_p^c(\mathbf{k}_{1\perp}) \left[f^i(\mathbf{p}_\perp) T_A^d U^{dc}(\mathbf{k}_{2\perp}) \right. \\ & \left. - \int \frac{d^2 \mathbf{k}_\perp}{(2\pi)^2} f^i(\mathbf{p}_\perp - \mathbf{k}_\perp) U(\mathbf{k}_\perp) T_A^c U^\dagger(\mathbf{k}_\perp - \mathbf{k}_{2\perp}) \right]. \end{aligned} \quad (83)$$

This production amplitude given in coordinate space exactly coincides with the third term of Eq. (5.8) in Ref. [9] except normalization. We should remark that Eq. (83) is independent of the rapidity difference Δy as we neglect $e^{-\Delta y}$ under the condition that only q^+ and p^- are dominating.

Next, we will consider a different situation with the rapidity dependence handled easily. Let \mathbf{p}_\perp and \mathbf{q}_\perp be much bigger than $\mathbf{k}_{1\perp}$, $\mathbf{k}_{2\perp}$, and \mathbf{k}_\perp . This means that \mathbf{p}_\perp and \mathbf{q}_\perp belong to the hard scale as compared to the saturation scale which characterizes the gluon distribution inside the target nucleus. We note that this situation is the case if we are interested in the di-jet correlations. We shall further limit our calculation here to the back-to-back kinematics, i.e.

$$\mathbf{p}_\perp + \mathbf{q}_\perp = \mathbf{k}_{1\perp} + \mathbf{k}_{2\perp} = \mathbf{0}_\perp, \quad (84)$$

for simplicity.

As a matter of fact, the back-to-back kinematics significantly reduces complexity enabling us to perform explicit calculations with a reasonable effort. Without any expansion we can express $T_{(>)}$ and $T_{(<)}$ as

$$\begin{aligned} T_{(>)}^{ij}(p, q; \mathbf{k}_{1\perp}, \mathbf{k}_{2\perp}) \\ = \frac{[\mathbf{k}_{1\perp}^2 \tanh(\Delta y/2) + 2\mathbf{k}_{1\perp} \cdot \mathbf{p}_\perp] g^{ij} + 2k_1^j p^i (1 + e^{-\Delta y}) + 2k_1^i p^j (1 + e^{\Delta y})}{\mathbf{p}_\perp^2 (1 + \cosh \Delta y)}, \end{aligned} \quad (85)$$

$$\begin{aligned} T_{(<)}^{ij}(p, q; \mathbf{p}_\perp - \mathbf{k}_\perp, \mathbf{k}_{1\perp} + \mathbf{k}_\perp - \mathbf{p}_\perp) \\ = - \frac{\mathbf{k}_{1\perp} \cdot (2\mathbf{p}_\perp - 2\mathbf{k}_\perp - \mathbf{k}_{1\perp}) g^{ij} + 2k_1^j (p^i - k^i) (1 + e^{-\Delta y}) + 2k_1^i (p^j - k^j - k_1^j) (1 + e^{\Delta y})}{(\mathbf{p}_\perp - \mathbf{k}_\perp)^2 (1 + e^{-\Delta y})/2 + (\mathbf{p}_\perp - \mathbf{k}_\perp - \mathbf{k}_{1\perp})^2 (1 + e^{\Delta y})/2}. \end{aligned} \quad (86)$$

Here it is easy to make sure that the above two expressions are to be transmuted to Eqs. (80) and (81) in the limit of $\Delta y \rightarrow \infty$. It is also manifest that $T_{(>)} + T_{(<)}$ is vanishing up to the first order in terms of $\mathbf{k}_{1\perp}$ and \mathbf{k}_\perp . Let us henceforth look more into the rapidity dependence to grasp a feeling from the above results.

We expand Eqs. (85) and (86) in terms of $\mathbf{k}_{1\perp}$ and \mathbf{k}_\perp keeping the quadratic

order. After tedious but straightforward calculations we can reach;

$$T^{ij} = T_{(>)}^{ij} + T_{(<)}^{ij} \approx \frac{2\mathbf{k}_{1\perp} \cdot \bar{\mathbf{k}}_{\perp} g^{ij} + 2k_1^i \bar{k}'^j (1 + e^{-\Delta y}) + 2k_1^j \bar{k}'^i (1 + e^{\Delta y})}{p_{\perp}^2 (1 + \cosh \Delta y)}, \quad (87)$$

where we define

$$\bar{\mathbf{k}}_{\perp} = \tilde{\mathbf{k}}_{\perp} - 2(\hat{\mathbf{p}}_{\perp} \cdot \tilde{\mathbf{k}}_{\perp}) \hat{\mathbf{p}}_{\perp}, \quad \tilde{\mathbf{k}}_{\perp} = \mathbf{k}_{\perp} + \frac{1}{1 + e^{-\Delta y}} \mathbf{k}_{1\perp}, \quad (88)$$

and $\hat{\mathbf{p}}_{\perp} = \mathbf{p}_{\perp}/|\mathbf{p}_{\perp}|$. The system having translational symmetry in the transverse plane constrains as $\mathbf{k}'_{1\perp} = \mathbf{k}_{1\perp}$, but not for \mathbf{k}_{\perp} and \mathbf{k}'_{\perp} . The squared quantity of the above matrix takes a relatively simple form of

$$\text{tr}[T \cdot T^{\dagger}] = \frac{8[(\mathbf{k}_{1\perp} \cdot \bar{\mathbf{k}}_{\perp})(\mathbf{k}_{1\perp} \cdot \bar{\mathbf{k}}'_{\perp}) + 2k_{1\perp}^2 (\bar{\mathbf{k}}_{\perp} \cdot \bar{\mathbf{k}}'_{\perp}) \cosh \Delta y (1 + \cosh \Delta y)]}{p_{\perp}^2 (1 + \cosh \Delta y)^2}. \quad (89)$$

Here the angular average with respect to $\hat{\mathbf{p}}_{\perp}$ can take us to make further simplification, so that we finally get

$$\text{tr}[T \cdot T^{\dagger}] = \frac{4\mathbf{k}_{1\perp}^2 (\tilde{\mathbf{k}}_{\perp} \cdot \tilde{\mathbf{k}}'_{\perp})}{p_{\perp}^2} \cdot \left(\frac{1 + 2 \cosh \Delta y}{1 + \cosh \Delta y} \right)^2. \quad (90)$$

Here we should not forget that $\tilde{\mathbf{k}}_{\perp}$ and $\tilde{\mathbf{k}}'_{\perp}$ have the rapidity dependence too. By shifting $\mathbf{k}_{\perp} \rightarrow \mathbf{k}_{\perp} - \mathbf{k}_{1\perp}/2$ and $\mathbf{k}'_{\perp} \rightarrow \mathbf{k}'_{\perp} - \mathbf{k}_{1\perp}/2$, the final expression for the back-to-back two-gluon production from the connected diagram is

$$\begin{aligned} \left\langle \frac{dN_{\text{gg}}}{d|\mathbf{p}_{\perp}| dy_1 dy_2} \Big|_{\mathbf{q}_{\perp} = -\mathbf{p}_{\perp}} \right\rangle_{\text{conn}} &= \frac{\alpha_s}{(N_c^2 - 1) \pi^2 p_{\perp}^2} \int \frac{d^2 \mathbf{k}_{1\perp}}{(2\pi)^2} \varphi_{\text{p}}(\mathbf{k}_{1\perp}) \\ &\times \int \frac{d^2 \mathbf{k}_{\perp}}{(2\pi)^2} \frac{d^2 \mathbf{k}'_{\perp}}{(2\pi)^2} \left[\mathbf{k}_{\perp} \cdot \mathbf{k}'_{\perp} + \frac{1}{4} (\tanh(\Delta y/2))^2 k_{1\perp}^2 \right] \cdot \left(\frac{1 + 2 \cosh \Delta y}{1 + \cosh \Delta y} \right)^2 \\ &\times \left\langle \text{tr}[U(\mathbf{k}_{\perp} - \mathbf{k}_{1\perp}/2) T_{\text{A}}^a U^{\dagger}(\mathbf{k}_{\perp} + \mathbf{k}_{1\perp}/2) U(\mathbf{k}'_{\perp} + \mathbf{k}_{1\perp}/2) T_{\text{A}}^a U^{\dagger}(\mathbf{k}'_{\perp} - \mathbf{k}_{1\perp}/2)] \right\rangle. \end{aligned} \quad (91)$$

Here we have used the gluon distribution function defined in Eq. (A.1) in Appendix A.

At this moment without the numerical integration involving the Wilson lines we cannot quantify the dependence on Δy in a clear way. Because $\mathbf{k}_{\perp} \cdot \mathbf{k}'_{\perp}$ is expected to have a value close to $\mathbf{k}_{1\perp}^2$ (if $\mathbf{k}_{1\perp}$ is absent the $\mathbf{k}_{\perp} \cdot \mathbf{k}'_{\perp}$ term does not survive after the momentum integration), we can parametrically infer the dependence by the functional form of

$$\left[\xi + \frac{1}{4} (\tanh(\Delta y/2))^2 \right] \cdot \left(\frac{1 + 2 \cosh \Delta y}{1 + \cosh \Delta y} \right)^2 \quad (92)$$

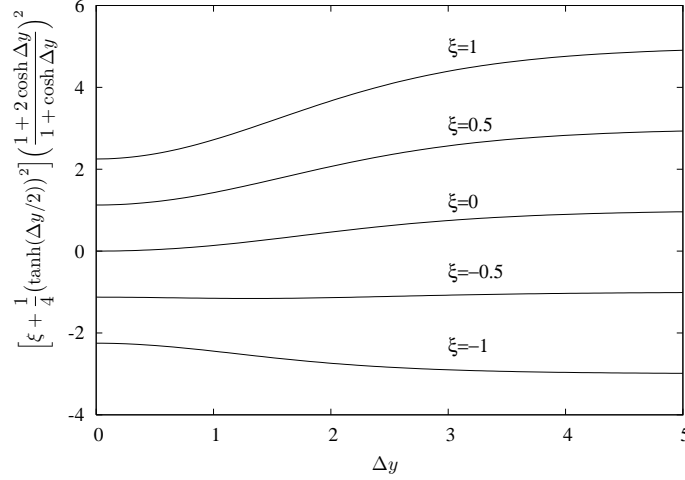


Fig. 5. Dependence on Δy for various values of the unknown parameter ξ .

with an unknown parameter ξ corresponding to the ratio between two terms proportional to $\mathbf{k}_\perp \cdot \mathbf{k}'_\perp$ and $\mathbf{k}_{1\perp}^2$, respectively. We plot the above function for $\xi = -1, -0.5, 0, 0.5, 1$, in Fig. 5.

Since ξ should presumably be positive due to the symmetric property of Eq. (91), our results in Fig. 5 claim that the connected diagram enhances the long range correlations in rapidity. Also we can see that the rapidity dependence is only moderate and no exponentially damping correlation appears.

6 Conclusions

We explicitly calculated the two-gluon multiplicity in the pA collision using the framework of the Color Glass Condensate and the LSZ reduction formula. We specifically choose a connected diagram which could be the only contribution to produce the intrinsic dependence on the longitudinal or rapidity separation between emitted gluons. To accomplish the calculation we wrote down the classical gluon field associated with the dilute and dense color sources and put it to the background propagator.

Our final results encompass the rapidity dependence that is not taken into account in the eikonal limit, but they are too complicated to perceive the qualitative behavior as a function of the rapidity separation. We have to wait for numerical evaluation, which we plan to do as a natural extension of this work, in order to extract phenomenological physics implication from our analytical expressions.

In this paper we proceeded to analyze the rapidity dependence in the special cases. First, we confirmed that our expressions are certainly reduced to the

expression given in Ref. [9] in the eikonal limit. Next, we relaxed this limit so as to allow for the rapidity separation under the condition that the momenta carried by emitted gluons are hard as compared to the gluon distribution in the projectile and target hadrons. In this case we found a fairly concise formula for the two-gluon production in the back-to-back kinematics. Our results imply that the dependence on the rapidity separation is only moderate and there arise no exponentially damping correlations.

In fact, our finding is the other way around; the connected diagram enhances the long range correlations in rapidity. That is, the contribution to the multiplicity from the connected diagram gets larger with increasing rapidity separation. Although this might sound curious at first, this could be possible because we consider two gluons split from one gluon. The long range correlations in this case simply signifies that more gluons come out with larger longitudinal angle. In fact, the three-point vertex in QCD contains $p^+/q^+ = e^{\Delta y}$ which surpasses the energy denominator. We remind that our tree-level description breaks down eventually for $\Delta y > 1/\alpha_2$ due to quantum effects.

It is quite interesting to see such long range correlations in rapidity and this observation seems to be consistent with the ridge phenomenon observed at RHIC. We cannot, of course, make any convincing statement about the near-side jet correlations from our rough analyses limited to the back-to-back kinetics. It is indispensable to perform the numerical integration to quantify the two-gluon production. In the near future we are planning to include the disconnected diagram, which is much simpler than the connected one we manipulated here, to discuss not only the rapidity dependence but also the azimuthal angle dependence and their interplay in this framework.

We thank Larry McLerran for encouraging us to initiate this problem. We thank François Gélis and Raju Venugopalan for discussions. K. F. is supported by Japanese MEXT grant no. 20740134 and also supported in part by Yukawa International Program for Quark Hadron Sciences.

A Appendix – Gluon Distributions

To make the final expression (78) more comprehensible in an intuitive way let us make use of the notation by the parton distribution functions along the similar line as Ref. [4]. We first define the proton unintegrated gluon distribution;

$$\begin{aligned} & \langle \rho_p^a(\mathbf{k}_{1\perp}) \rho_p^{a'*}(\mathbf{k}'_{1\perp}) \rangle \\ &= \frac{\delta^{aa'}}{\pi(N_c^2 - 1)} \left(\frac{\mathbf{k}_{1\perp} + \mathbf{k}'_{1\perp}}{2} \right)^2 \int d^2 \mathbf{X}_\perp e^{i(\mathbf{k}_{1\perp} - \mathbf{k}'_{1\perp}) \cdot \mathbf{X}_\perp} \frac{d\varphi_p\left(\frac{\mathbf{k}_{1\perp} + \mathbf{k}'_{1\perp}}{2} | \mathbf{X}_\perp\right)}{d^2 \mathbf{X}_\perp}. \end{aligned} \quad (\text{A.1})$$

The above equality could be understood as the definition for $\varphi_p(\mathbf{k}_\perp|\mathbf{X}_\perp)$. It is a straightforward generalization to proceed to the definition for the two-point correlator, that is,

$$\begin{aligned} \delta^{aa'} \langle U^{ba}(\mathbf{k}_{2\perp}) U^{\dagger a'b'}(\mathbf{k}'_{2\perp}) \text{tr}[T_A^b T_A^{b'}] \rangle &= N_c \langle \text{tr}[U(\mathbf{k}_{2\perp}) U^\dagger(\mathbf{k}'_{2\perp})] \rangle \\ &= \frac{g^2 N_c^2}{\pi \mathbf{k}_{2\perp}^2} \int d^2 \mathbf{X}_\perp e^{i(\mathbf{k}_{2\perp} - \mathbf{k}'_{2\perp}) \cdot \mathbf{X}_\perp} \frac{d\varphi_A^{g,g}(\mathbf{k}_{2\perp}|\mathbf{X}_\perp - \mathbf{b})}{d^2 \mathbf{X}_\perp}. \end{aligned} \quad (\text{A.2})$$

We should note that \mathbf{b} is the impact parameter that specifies the relative separation from the proton gluon distribution in the transverse plane. The three-point correlator goes on to be

$$\begin{aligned} \delta^{aa'} \langle \text{tr}[U(\mathbf{k}_\perp) T_A^a U^\dagger(\mathbf{k}_\perp - \mathbf{k}_{2\perp}) T_A^{b'}] U^{\dagger a'b'}(\mathbf{k}'_{2\perp}) \rangle \\ = \frac{g^2 N_c^2}{\pi \mathbf{k}_{2\perp}^2} \int d^2 \mathbf{X}_\perp e^{i(\mathbf{k}_{2\perp} - \mathbf{k}'_{2\perp}) \cdot \mathbf{X}_\perp} \frac{d\varphi_A^{gg,g}(\mathbf{k}_\perp, \mathbf{k}_{2\perp} - \mathbf{k}_\perp; \mathbf{k}_{2\perp}|\mathbf{X}_\perp - \mathbf{b})}{d^2 \mathbf{X}_\perp}. \end{aligned} \quad (\text{A.3})$$

The four-point correlator is

$$\begin{aligned} \delta^{aa'} \langle \text{tr}[U(\mathbf{k}_\perp) T_A^a U^\dagger(\mathbf{k}_\perp - \mathbf{k}_{2\perp}) U(\mathbf{k}'_\perp - \mathbf{k}'_{2\perp}) T_A^{a'} U^\dagger(\mathbf{k}'_\perp)] \rangle \\ = \frac{g^2 N_c^2}{\pi \mathbf{k}_{2\perp}^2} \int d^2 \mathbf{X}_\perp e^{i(\mathbf{k}_{2\perp} - \mathbf{k}'_{2\perp}) \cdot \mathbf{X}_\perp} \frac{d\varphi_A^{gg,gg}(\mathbf{k}_\perp, \mathbf{k}_{2\perp} - \mathbf{k}_\perp; \mathbf{k}'_\perp, \mathbf{k}'_{2\perp} - \mathbf{k}'_\perp|\mathbf{X}_\perp - \mathbf{b})}{d^2 \mathbf{X}_\perp}. \end{aligned} \quad (\text{A.4})$$

Here we assume that the distribution functions are approximately homogeneous in transverse space, which is often the case in the McLerran-Venugopalan model treatment based on the Gaussian distribution for the color source. Then, the integration over the transverse plane gives rise to the momentum delta functions, which simplifies the final results to be

$$\begin{aligned} \left\langle \frac{dN_{\text{gg}}}{dy_1 dy_2} \right\rangle_{\text{conn}} &= \frac{\alpha_s^2 N_c^2}{(N_c^2 - 1) \pi^2} \int \frac{d^2 \mathbf{p}_\perp}{(2\pi)^2} \frac{d^2 \mathbf{q}_\perp}{(2\pi)^2} \frac{d^2 \mathbf{k}_{1\perp}}{(2\pi)^2} \frac{\varphi_p(\mathbf{k}_{1\perp})}{\mathbf{k}_{1\perp}^2 \mathbf{k}_{2\perp}^2} \\ &\times \left\{ \text{tr}[T_{(>)} \cdot T_{(>)}^\dagger] \varphi_A^{g,g}(\mathbf{k}_{2\perp}) + \int \frac{d^2 \mathbf{k}_\perp}{(2\pi)^2} \text{tr}[T_{(<)} \cdot T_{(>)}^\dagger] \varphi_A^{gg,g}(\mathbf{k}_\perp, \mathbf{k}_{2\perp} - \mathbf{k}_\perp; \mathbf{k}_{2\perp}) \right. \\ &+ \int \frac{d^2 \mathbf{k}'_\perp}{(2\pi)^2} \text{tr}[T_{(>)} \cdot T_{(<)}^\dagger] \varphi_A^{gg,g}(\mathbf{k}_\perp, \mathbf{k}_{2\perp} - \mathbf{k}_\perp; \mathbf{k}_{2\perp}) \\ &\left. + \int \frac{d^2 \mathbf{k}_\perp}{(2\pi)^2} \frac{d^2 \mathbf{k}'_\perp}{(2\pi)^2} \text{tr}[T_{(<)} \cdot T_{(<)}^\dagger] \varphi_A^{gg,gg}(\mathbf{k}_\perp, \mathbf{k}_{2\perp} - \mathbf{k}_\perp; \mathbf{k}'_\perp, \mathbf{k}_{2\perp} - \mathbf{k}'_\perp) \right\}. \end{aligned} \quad (\text{A.5})$$

It is necessary to calculate the gluon distribution functions for numerical evaluation and we can utilize the McLerran-Venugopalan model. Appendix B is devoted to the explanation of how to compute the average of the Wilson lines.

B Appendix – Average of the Wilson Lines

In this appendix, we evaluate the Gaussian average for the two-, three- and four-point functions in terms of the Wilson line in the adjoint representation. They are all necessary to compute the gluon distribution functions in the McLerran-Venugopalan model. For this purpose it is enough to calculate the four-point function because the two- and three-point functions are readily deduced by the appropriate contraction from the four-point function as

$$N_c \langle \text{tr}[U(\mathbf{x}_{1\perp})U^\dagger(\mathbf{x}_{2\perp})] \rangle = \langle \text{tr}[U(\mathbf{x}_{1\perp})T_A^a U^\dagger(\mathbf{x}_{3\perp})U(\mathbf{x}_{3\perp})T_A^a U^\dagger(\mathbf{x}_{2\perp})] \rangle, \quad (\text{B.1})$$

and

$$\begin{aligned} & \langle \text{tr}[U(\mathbf{x}_{1\perp})T_A^a U^\dagger(\mathbf{x}_{2\perp})T_A^b U^{\dagger ab}(\mathbf{x}_{3\perp})] \rangle \\ &= \langle \text{tr}[U(\mathbf{x}_{1\perp})T_A^a U^\dagger(\mathbf{x}_{2\perp})U(\mathbf{x}_{3\perp})T_A^a U^\dagger(\mathbf{x}_{3\perp})] \rangle. \end{aligned} \quad (\text{B.2})$$

Calculating the generic four-point function in the adjoint representation is a tedious task, though it is not impossible. Instead, we thus adopt the large- N_c expansion here. We can express the adjoint Wilson line using the fundamental Wilson lines as

$$U(\mathbf{x}_{i\perp})_{\beta\alpha} = 2\text{tr}[T_F^\beta U_F(\mathbf{x}_{i\perp})T_F^\alpha U_F^\dagger(\mathbf{x}_{i\perp})], \quad (\text{B.3})$$

where $U_F(\mathbf{x}_{i\perp})$ is the fundamental Wilson line and T_F is the generator in the fundamental representation. Using Eq. (B.3) we can then rewrite the four-point function in the adjoint representation as follows;

$$\begin{aligned} & \langle \text{tr}[U(\mathbf{x}_{1\perp})T_A^a U^\dagger(\mathbf{x}_{2\perp})U(\mathbf{x}_{3\perp})T_A^a U^\dagger(\mathbf{x}_{4\perp})] \rangle \\ &= 4T_{A\alpha_1\alpha_2}^a T_{A\alpha_3\alpha_4}^a T_F^{\alpha_1}_{a_1\bar{a}_1} T_F^{\alpha_2}_{a_2\bar{a}_2} T_F^{\alpha_3}_{a_3\bar{a}_3} T_F^{\alpha_4}_{a_4\bar{a}_4} \\ & \quad \times 4\delta_{\beta_1\beta_4}\delta_{\beta_2\beta_3} T_F^{\beta_1}_{b_1\bar{b}_1} T_F^{\beta_2}_{b_2\bar{b}_2} T_F^{\beta_3}_{b_3\bar{b}_3} T_F^{\beta_4}_{b_4\bar{b}_4} \left\langle \prod_{i=1}^4 U_{Fb_i a_i}(\mathbf{x}_{i\perp}) U_{F\bar{b}_i \bar{a}_i}^*(\mathbf{x}_{i\perp}) \right\rangle. \end{aligned} \quad (\text{B.4})$$

In the same way as the present authors did in Ref. [24] we shall introduce the “initial state” and the “final state” as

$$\begin{aligned} \langle a_1, a_2, a_3, a_4, \bar{a}_1, \bar{a}_2, \bar{a}_3, \bar{a}_4 | \text{initial} \rangle &= 4T_{A\alpha_1\alpha_2}^a T_{A\alpha_3\alpha_4}^a T_F^{\alpha_1}_{a_1\bar{a}_1} T_F^{\alpha_2}_{a_2\bar{a}_2} T_F^{\alpha_3}_{a_3\bar{a}_3} T_F^{\alpha_4}_{a_4\bar{a}_4} \\ &= \frac{1}{2} \left(\delta_{a_1\bar{a}_4} \delta_{a_2\bar{a}_1} \delta_{a_3\bar{a}_2} \delta_{a_4\bar{a}_3} + \delta_{a_1\bar{a}_2} \delta_{a_2\bar{a}_3} \delta_{a_3\bar{a}_4} \delta_{a_4\bar{a}_1} \right. \\ & \quad \left. - \delta_{a_1\bar{a}_3} \delta_{a_2\bar{a}_1} \delta_{a_3\bar{a}_4} \delta_{a_4\bar{a}_2} - \delta_{a_1\bar{a}_2} \delta_{a_2\bar{a}_4} \delta_{a_3\bar{a}_1} \delta_{a_4\bar{a}_3} \right), \end{aligned} \quad (\text{B.5})$$

$$\begin{aligned} \langle \text{final} | b_1, b_2, b_3, b_4, \bar{b}_1, \bar{b}_2, \bar{b}_3, \bar{b}_4 \rangle &= 4\delta_{\beta_1\beta_4}\delta_{\beta_2\beta_3} T_F^{\beta_1}_{b_1\bar{b}_1} T_F^{\beta_2}_{b_2\bar{b}_2} T_F^{\beta_3}_{b_3\bar{b}_3} T_F^{\beta_4}_{b_4\bar{b}_4} \\ &= \delta_{b_1\bar{b}_4} \delta_{b_2\bar{b}_3} \delta_{b_3\bar{b}_2} \delta_{b_4\bar{b}_1} + \frac{1}{N_c^2} \delta_{b_1\bar{b}_1} \delta_{b_2\bar{b}_2} \delta_{b_3\bar{b}_3} \delta_{b_4\bar{b}_4} \\ & \quad - \frac{1}{N_c} \left(\delta_{b_1\bar{b}_1} \delta_{b_2\bar{b}_3} \delta_{b_3\bar{b}_2} \delta_{b_4\bar{b}_4} + \delta_{b_1\bar{b}_4} \delta_{b_2\bar{b}_2} \delta_{b_3\bar{b}_3} \delta_{b_4\bar{b}_1} \right), \end{aligned} \quad (\text{B.6})$$

and also define the “Hamiltonian” composed of the free part, H_0 , and the interaction V ;

$$H_0 = \frac{Q_s'^2}{N_c} L(0, 0) \left[\sum_{i=1}^4 (T_{F_i}^a - T_{F_i}^{a*}) \right]^2, \quad (\text{B.7})$$

$$V = -\frac{Q_s'^2}{N_c} \left\{ \sum_{i>j}^4 \left[T_{F_i}^a T_{F_j}^a \Gamma(\mathbf{x}_{i\perp}, \mathbf{x}_{j\perp}) + T_{F_i}^{a*} T_{F_j}^{a*} \Gamma(\mathbf{x}_{i\perp}, \mathbf{x}_{j\perp}) \right] - \sum_{i,j=1}^4 T_{F_i}^a T_{F_j}^{a*} \Gamma(\mathbf{x}_{i\perp}, \mathbf{x}_{j\perp}) \right\}, \quad (\text{B.8})$$

where we use the same notation as in Ref. [24] as

$$\begin{aligned} L(\mathbf{x}_{1\perp}, \mathbf{x}_{2\perp}) &= g^4 \int d^2 \mathbf{z}_{\perp} G_0(\mathbf{x}_{1\perp} - \mathbf{z}_{\perp}) G_0(\mathbf{x}_{2\perp} - \mathbf{z}_{\perp}), \\ \Gamma(\mathbf{x}_{1\perp}, \mathbf{x}_{2\perp}) &= 2L(0, 0) - 2L(\mathbf{x}_{1\perp}, \mathbf{x}_{2\perp}). \end{aligned} \quad (\text{B.9})$$

Here $G_0(\mathbf{x}_{\perp} - \mathbf{z}_{\perp})$ is the propagator in two dimensions satisfying $\partial_{\perp}^2 G_0(\mathbf{x}_{\perp} - \mathbf{z}_{\perp}) = \delta^{(2)}(\mathbf{x}_{\perp} - \mathbf{z}_{\perp})$. We note that the saturation scale Q_s' has a different normalization from Ref. [24], that is, we have defined $Q_s'^2 = 2N_c^2/(N_c^2 - 1)Q_s^2$. By means of the bra- and ket-vectors, the initial and final states become

$$\begin{aligned} |\text{initial}\rangle &= \frac{1}{2} N_c^2 (|4123\rangle + |2341\rangle - |3142\rangle - |2413\rangle), \\ \langle \text{final}| &= N_c^2 \langle 4321| + \langle 1234| - N_c \langle 1324| - N_c \langle 4231|, \end{aligned}$$

where we define

$$\langle a_1, a_2, a_3, a_4, \bar{a}_1, \bar{a}_2, \bar{a}_3, \bar{a}_4 |ijkl\rangle = \frac{1}{N_c^2} \delta_{a_1 \bar{a}_i} \delta_{a_2 \bar{a}_j} \delta_{a_3 \bar{a}_k} \delta_{a_4 \bar{a}_l}, \quad (\text{B.10})$$

whose norm is normalized properly to unity. Here we note that $|ijkl\rangle$'s form a complete set of the singlet states out of $N_c \otimes N_c^* \otimes N_c \otimes N_c^* \otimes N_c \otimes N_c^* \otimes N_c \otimes N_c^*$, that is, satisfy $H_0 |ijkl\rangle = 0$, though $|ijkl\rangle$ is not the orthogonal basis.

Let us consider the large- N_c limit and then one might naïvely think that the leading order of the matrix element would be $\mathcal{O}(N_c^4)$ since both the initial and final states are $\mathcal{O}(N_c^2)$. This is, however, not true. In the large- N_c limit V is diagonal and $\langle \text{final} | \text{initial} \rangle = \mathcal{O}(N_c^3)$ [24, 13]. Unfortunately, since the leading-order contribution vanishes, we need to calculate the next-to-leading order in the large N_c expansion.

For the purpose of proceeding to the next-to-leading order, we need to know

the overlap between different states. These are directly read as

$$\begin{aligned}\langle 4321|4123\rangle &= \langle 4321|2341\rangle = \frac{1}{N_c}, \\ \langle 4321|3142\rangle &= \langle 4321|2413\rangle = \frac{1}{N_c^2}.\end{aligned}\tag{B.11}$$

As we mentioned above, the matrix elements of e^{-V} are $\mathcal{O}(1)$ for the (vanishing) diagonal components and are $\mathcal{O}(1/N_c)$ for the off-diagonal components. Hence the only first equation in Eq. (B.11) gives a finite contribution to the next-to-leading order, while the second one is the next-to-next-to-leading order in this counting.

As a result of the truncation up to $\mathcal{O}(N_c^3)$ the matrix element is expressed as

$$\langle \text{final}|e^{-V}|\text{initial}\rangle \simeq \frac{N_c^4}{2} \left(\langle 4321|e^{-V}|4123\rangle + \langle 4321|e^{-V}|2341\rangle \right). \tag{B.12}$$

Henceforth, let us focus on the evaluation of $\langle 4321|e^{-V}|4123\rangle$ appearing in Eq. (B.12). By definition e^{-V} is expanded as

$$e^{-V} = \sum_{n=0}^{\infty} \frac{(-1)^n}{n!} V^n. \tag{B.13}$$

We shall operate V onto $|4123\rangle$ and $|4321\rangle$. Using the diagrammatical technique developed in Ref. [24] we can find,

$$\begin{aligned}V|4123\rangle &= V_{11}|4123\rangle + \frac{1}{N_c}V_{21}|4321\rangle + \dots, \\ V|4321\rangle &= V_{22}|4321\rangle + \dots,\end{aligned}\tag{B.14}$$

where

$$\begin{aligned}V_{11} &= \frac{Q_s^2}{2} \left[\Gamma(\mathbf{x}_{1\perp}, \mathbf{x}_{2\perp}) + \Gamma(\mathbf{x}_{2\perp}, \mathbf{x}_{3\perp}) + \Gamma(\mathbf{x}_{3\perp}, \mathbf{x}_{4\perp}) + \Gamma(\mathbf{x}_{1\perp}, \mathbf{x}_{4\perp}) \right], \\ V_{21} &= \frac{Q_s^2}{2} \left[\Gamma(\mathbf{x}_{1\perp}, \mathbf{x}_{4\perp}) + \Gamma(\mathbf{x}_{2\perp}, \mathbf{x}_{3\perp}) - \Gamma(\mathbf{x}_{2\perp}, \mathbf{x}_{4\perp}) - \Gamma(\mathbf{x}_{1\perp}, \mathbf{x}_{3\perp}) \right], \\ V_{22} &= \frac{Q_s^2}{2} \left[2\Gamma(\mathbf{x}_{1\perp}, \mathbf{x}_{4\perp}) + 2\Gamma(\mathbf{x}_{2\perp}, \mathbf{x}_{3\perp}) \right].\end{aligned}\tag{B.15}$$

Here the ellipsis “ \dots ” in Eq. (B.14) represents sub-leading states such as $|3142\rangle$, $|2413\rangle$, and so on, which are higher order. We can go on this procedure to make V^n act onto $|4123\rangle$, and then we get the following;

$$\begin{aligned}V^n|4123\rangle &= |4123\rangle V_{11}^n + \frac{1}{N_c}|4321\rangle V_{21}(V_{11}^{n-1} + V_{22}V_{11}^{n-2} + \dots + V_{22}^{n-1}) + \dots \\ &= |4123\rangle V_{11}^n + \frac{1}{N_c}|4321\rangle V_{21} \frac{V_{11}^n - V_{22}^n}{V_{11} - V_{22}} + \dots.\end{aligned}\tag{B.16}$$

Consequently the necessary matrix element is acquired as

$$\langle 4321|e^{-V}|4123\rangle = \frac{1}{N_c}e^{-V_{11}} + \frac{1}{N_c}\frac{V_{21}}{V_{11}-V_{22}}(e^{-V_{11}} - e^{-V_{22}}) + \mathcal{O}\left(\frac{1}{N_c^2}\right). \quad (\text{B.17})$$

We take the same path to evaluate $\langle 4321|e^{-V}|2341\rangle$ only to find that

$$\langle 4321|e^{-V}|2341\rangle = \langle 4321|e^{-V}|4123\rangle. \quad (\text{B.18})$$

Finally we reach the answer,

$$\begin{aligned} & \left\langle \text{tr}[U(\mathbf{x}_{1\perp})T_A^a U^\dagger(\mathbf{x}_{2\perp})U(\mathbf{x}_{3\perp})T_A^a U^\dagger(\mathbf{x}_{4\perp})] \right\rangle \\ &= \langle \text{final}|e^{-V}|\text{initial}\rangle = N_c^3 \left[e^{-V_{11}} + \frac{V_{21}}{V_{11}-V_{22}}(e^{-V_{11}} - e^{-V_{22}}) \right]. \end{aligned} \quad (\text{B.19})$$

Now that we have the four-point function, it is straightforward to evaluate the two- and three-point functions by substituting $(\mathbf{x}_{2\perp} \rightarrow \mathbf{x}_{3\perp}, \mathbf{x}_{4\perp} \rightarrow \mathbf{x}_{2\perp})$ and $\mathbf{x}_{4\perp} \rightarrow \mathbf{x}_{3\perp}$, respectively. That is,

$$N_c \left\langle \text{tr}[U(\mathbf{x}_{1\perp})U^\dagger(\mathbf{x}_{2\perp})] \right\rangle = N_c^3 e^{-V_{22}} = N_c^3 e^{-Q_s'^2 \Gamma(\mathbf{x}_{1\perp}, \mathbf{x}_{2\perp})}, \quad (\text{B.20})$$

and

$$\begin{aligned} & \left\langle \text{tr}[U(\mathbf{x}_{1\perp})T_A^a U^\dagger(\mathbf{x}_{2\perp})T_A^b U^\dagger(\mathbf{x}_{3\perp})] \right\rangle \\ &= N_c^3 e^{-V_{22}} = N_c^3 e^{-\frac{1}{2}Q_s'^2 [\Gamma(\mathbf{x}_{1\perp}, \mathbf{x}_{2\perp}) + \Gamma(\mathbf{x}_{2\perp}, \mathbf{x}_{3\perp}) + \Gamma(\mathbf{x}_{1\perp}, \mathbf{x}_{3\perp})]}. \end{aligned} \quad (\text{B.21})$$

Although these results for the two- and three-point functions are limited to large N_c , we can reproduce the correct answer by replacing N_c^3 by $N_c(N_c^2 - 1)$ in view of the results available from Refs. [27,24].

References

- [1] L. V. Gribov, E. M. Levin and M. G. Ryskin, Phys. Rept. **100**, 1 (1983); E. Gotsman, E. M. Levin and U. Maor, Phys. Lett. B **379**, 186 (1996) [arXiv:hep-ph/9512316].
- [2] L. D. McLerran and R. Venugopalan, Phys. Rev. D **49**, 2233 (1994) [arXiv:hep-ph/9309289]; *ibid.* D **49**, 3352 (1994) [arXiv:hep-ph/9311205]; *ibid.* D **50**, 2225 (1994) [arXiv:hep-ph/9402335].
- [3] For reviews, see: E. Iancu, A. Leonidov and L. McLerran, arXiv:hep-ph/0202270; E. Iancu and R. Venugopalan, arXiv:hep-ph/0303204; F. Gelis and R. Venugopalan, arXiv:hep-ph/0611157.
- [4] J. P. Blaizot, F. Gelis and R. Venugopalan, Nucl. Phys. A **743**, 13 (2004) [arXiv:hep-ph/0402256]; J. P. Blaizot, F. Gelis and R. Venugopalan, *ibid.* A **743**, 57 (2004) [arXiv:hep-ph/0402257].

- [5] E. Iancu, K. Itakura and L. McLerran, Nucl. Phys. A **724**, 181 (2003) [arXiv:hep-ph/0212123].
- [6] F. Gelis, T. Lappi and R. Venugopalan, arXiv:0804.2630 [hep-ph].
- [7] F. Gelis and Y. Mehtar-Tani, Phys. Rev. D **73**, 034019 (2006) [arXiv:hep-ph/0512079].
- [8] J. Jalilian-Marian and Y. V. Kovchegov, Phys. Rev. D **70**, 114017 (2004) [Erratum-ibid. D **71**, 079901 (2005)] [arXiv:hep-ph/0405266].
- [9] R. Baier, A. Kovner, M. Nardi and U. A. Wiedemann, Phys. Rev. D **72**, 094013 (2005) [arXiv:hep-ph/0506126].
- [10] T. Lappi and L. McLerran, Nucl. Phys. A **772**, 200 (2006) [arXiv:hep-ph/0602189].
- [11] A. Kovner, L. D. McLerran and H. Weigert, Phys. Rev. D **52**, 6231 (1995) [arXiv:hep-ph/9502289].
- [12] D. Kharzeev, E. Levin and L. McLerran, Nucl. Phys. A **748**, 627 (2005) [arXiv:hep-ph/0403271].
- [13] C. Marquet, Nucl. Phys. A **796**, 41 (2007) [arXiv:0708.0231 [hep-ph]].
- [14] A. Majumder, B. Muller and S. A. Bass, Phys. Rev. Lett. **99**, 042301 (2007) [arXiv:hep-ph/0611135].
- [15] A. Dumitru, F. Gelis, L. McLerran and R. Venugopalan, arXiv:0804.3858 [hep-ph].
- [16] N. Armesto, L. McLerran and C. Pajares, Nucl. Phys. A **781**, 201 (2007) [arXiv:hep-ph/0607345].
- [17] N. Armesto, M. A. Braun and C. Pajares, Phys. Rev. C **75**, 054902 (2007) [arXiv:hep-ph/0702216].
- [18] For a textbook, see; M. E. Peskin and D. V. Schroeder, “An Introduction To Quantum Field Theory,” Chap. 7.2, (*USA, Addison-Wesley, 1995, 842 p*).
- [19] P. P. Srivastava and S. J. Brodsky, Phys. Rev. D **64** (2001) 045006 [arXiv:hep-ph/0011372].
- [20] Y. Hatta, Nucl. Phys. A **781**, 104 (2007) [arXiv:hep-ph/0607126].
- [21] F. Gelis and R. Venugopalan, Nucl. Phys. A **776**, 135 (2006) [arXiv:hep-ph/0601209]; *ibid.* A **779**, 177 (2006) [arXiv:hep-ph/0605246].
- [22] Y. V. Kovchegov, Phys. Rev. D **54**, 5463 (1996) [arXiv:hep-ph/9605446].
- [23] T. Lappi, Phys. Rev. C **67**, 054903 (2003) [arXiv:hep-ph/0303076].
- [24] K. Fukushima and Y. Hidaka, JHEP **0706** (2007) 040 [arXiv:0704.2806 [hep-ph]].

- [25] K. Fukushima, Phys. Rev. D **77**, 074005 (2008) [arXiv:0711.2364 [hep-ph]].
- [26] A. Dumitru and L. D. McLerran, Nucl. Phys. A **700**, 492 (2002) [arXiv:hep-ph/0105268].
- [27] A. Kovner and U. A. Wiedemann, Phys. Rev. D **64** (2001) 114002 [arXiv:hep-ph/0106240].